PRESCOTT AIRPORT SOLAR FACILITY
SOLAR VARIABILITY STUDY

PERFORMED BY

Arizona Public Service
Northern Arizona University
3Tier, Inc.

Co-Authors:

Ronald K. Flood, Senior Consulting Engineer, Arizona Public Service
Dr. Tom Acker, Northern Arizona University, Institute for Sustainable Energy Solutions
David Willy, Graduate Research Assistant, Northern Arizona University
Jeff Lerner and Amy Vandervoort, 3Tier, Inc.

PREFACE

The purpose of this study was to familiarize APS with methods to measure, collect, store, and analyze critical data necessary to evaluate the behavior of solar irradiance on a solar facility and the output of the resulting power. While published techniques were used in much of the evaluation, new techniques have been introduced and evaluated for effectiveness. Coincident with the variability analysis, the evaluation of different methods for solar forecasting were also conducted.

This report is the joint effort between Arizona Public Service, Northern Arizona University, and 3Tier, Inc.

The contributing authors to this report were:

Ronald K. Flood, Senior Consulting Engineer, Arizona Public Service, Principal Investigator
Dr. Tom Acker, Professor of Mechanical Engineering, Northern Arizona University
David Willy, Graduate Research Assistant, Northern Arizona University
Amy Vandervoort, Director of Products and Projects, 3Tier, Inc.
Jeff Lerner, Director of Product Delivery, 3Tier, Inc.

The co-authors would like to acknowledge and thank Joshua S. Stein, Principle Member of Technical Staff, Sandia National Labs for valuable assistance with review and recommendations concerning analysis variables.

The co-authors would also like to thank Andrew Mills, Principal Research Associate, Lawrence Berkeley National Labs for his review, comment, and assistance for this document.

Special thanks for their contributions and research to Dr. Allison Kipple, Assistant Professor, Dept. of Electrical Engineering, Northern Arizona University, and Graduate Students, Santosh Chalise and Nazmul Arefin.

TABLE OF CONTENTS

LIST OF FIGURES

LIST OF TABLES

I. INTRODUCTION

Background

Over the past few years, a significant amount of photovoltaic (PV) solar production has been added to both the transmission and distribution grids. Residential and commercial PV additions result in a supplement of energy to the individual customer, in other words, a reduction of use of energy from the host utility. The utility, on the other hand, will experience a reduced load from the individual customer as the solar irradiance increases for more energy production on the individual customer PV. As more and more of these distributed resources are added to the system, the utility will experience a lower load than if there were no PV distributed resources as well as lower load ramp rates for "good solar resource" days. However, as more PV is added to any given distribution system, there is a higher potential for irradiance variability to be transferred as load variability into the distribution system with possible effects on the system voltage.

Recently, centralized photovoltaic facilities are being added in greater numbers. These systems are categorized as utility scale PV facilities and can range in sizes of 3 to 50 MW, or more depending on the available property and the capability of the utility to use this energy on any given power line. A very few of these facilities are interconnected to transmission lines, but the greater majority are being interconnected to distribution systems or small, radial transmission. These facilities are considered generators and provide additional resource energy into the power grid depending on the amount of solar irradiance resource available at the time.

Thus with the growth of photovoltaic, or the larger the penetration of the solar resource to the grid, the larger the effects experienced on the utility grid whether it be load related or generation related. With all types of the photovoltaic facilities, whether the aggregated, distributed/ customer PV or the centralized utility scale PV, a variability of energy is induced into the system to which it is interconnected. The first type of variability is a slower acting energy change induced by the position of the sun at any time of day and the amount of the energy available will be dependent on the time of the year. So as the sun goes up or the sun goes down, energy produced by the panel correlates. Average energy at any given time of the day can be reduced by other atmospheric conditions such as cloud cover, aerosols, and particulates. These effects reduce the amount of irradiance from the sun reaching the PV panel to produce the energy.

Moisture, aerosols, particulates and other dispersants can also induce high frequency variability as these atmospheric contaminants interfere with the solar irradiation reaching the solar panels. It should be noted that even with visual observation it can be difficult to determine if these dispersants are present along with the clouds particularly with storm conditions that can create both. This study, while recognizing that some of the power

output variability may be caused by conditions other than clouds, focuses only on observed cloud conditions.

The electric grid, whether transmission or distribution systems, is designed to provide energy to the load using available generation. Load varies throughout the day, and available generators will be ordered to increase or decrease their energy output to match the needs of the load demand. But load demand also is affected by the type and characteristic of the loads on the system and can result in characteristics with voltage or frequency variations. Since this variability can deteriorate the quality of the power being provided to the customers, generators also provide a service called increases or decreases generation relative to the scheduled amount at a high rate to compensate for these load effects. At the distribution level, other engineering devices will also provide some control to assure the power quality at the feeder level is maintained. The substation transformer is designed to not only meet the load requirement of each feeder for the substation but also provide regulation of the voltage for those feeders. Some loads may challenge the ability of the transformer to accomplish this, so localized voltage control devices are put in place such as switchable capacitors and variable voltage regulators.

As the penetration of the variable photovoltaic resources increase, the variability of energy increases at the points of the interconnection and eventually, across the power line to which they are connected. Since many of the resources are being connected to the distribution systems, these systems may be challenged before the resources begin to impact transmission systems.

Purpose of the Study

- Evaluate different techniques for analyzing variability
- Gain experience with analytic instrumentation and tools
- Determine the correlations with irradiance to the overall output
- Observe the effects of variability on the distribution system voltage
- Provide raw data to support additional studies considered by APS
- Determine any further issues that may need studied in the additional studies considered by APS
- Provide limited opportunity for comparisons of solar forecasts to actual performance

A large consideration for this study was that APS has had very limited experience at gathering and managing data at a high resolution. This was a preliminary study to determine a usable configuration for the data collection, the transmittal of this information into the APS data network, store the data in an easily retrievable method, and analyze the data to provide meaningful information. APS also evaluated information from already installed electrical measurement devices in the distribution systems, to determine the value of this information. The methodologies were then used in designing other data systems for use in more advanced APS studies. Since high resolution data is scarce in the industry, a 1-second resolution was selected. This

resolution allowed for an analysis of the question: What is the best resolution to analyze solar irradiance for variability? The high resolution also allowed for finer detail for the differences seen at various parts of the solar field at any given time.

In addition to the collection and management of data, it was suggested that current methods of analyzing variability might be augmented with additional techniques. Northern Arizona University worked closely with APS both in data design and then in providing analysis techniques around the data. Some new techniques have been developed and herein are compared with existing methods.

Since the tools for solar forecasting are still under development to improve to a level being achieved by wind forecasting, 3Tier, Inc. also participated in the study and provided a day ahead forecast of PV production. The day ahead forecast was then compared to actual performance conditions. During the study, a variety of different forecasting methods was employed to evaluate the accuracy of each or the conditions for which each method worked the best. Although much of the result of this portion of the study has been withheld as proprietary, 3Tier has provided a summary of the results for this publication, and APS has learned more about the value and the limitations of current solar forecasting.

The following activities and analyses were performed for this study:

- Determine test equipment setup and data collection, storage, and retrieval methods to provide better data availability for future APS studies.
- Measure the irradiance provided to one solar facility. These measurements are to be taken at rate sufficient to determine variation in irradiance conditions caused by clouds.
- Determine what data collection rate provides good characterization of variance caused by cloud conditions. For this reason, data was collected at 1-second.
- Determine the effects of various irradiance conditions on the power produced by the PV facility.
- Observe the irradiance ramp rates with the variations and correlate with the power ramp rates.
    - Observe the effects, if any, on the feeder voltages.
    - Observe the effects, if any, on power ramp rates due to the size of the facility (geographic dispersion)
- Provide a daily forecast for the facility showing hourly patterns.
    - Observe the accuracy of the forecast.
    - Using actual data, improve forecasting accuracy and methodology.
    - Provide recommendations on the use of historical data and anticipated weather conditions to improve power forecast.

Summary of Findings

- This project provided good experience in setting up test equipment for a solar facility and learning about new instrumentation and communication links for use in future projects.
- It helped APS learn how to manage large quantities of data in a manner that was retrievable and in a format that allowed for quality analysis. The methodology used in this project was used in designing data retrieval and management for other renewable projects.
- Since irradiation and power ramp evaluation is important for solar resources, it was found that the closer to one second data collection that could be achieved, the more accurate the evaluation.
- Averaging, even with short interval data, results in minimizing key information on the nature of the peaks of the variability and can result in misrepresenting the true impact of the variability of the irradiance on the output of the facility.
- A new methodology with new terms was introduced which may provide improvement in the analysis of irradiance and power variability for a given array or for any facility. These terms demonstrated improvement over Clear Sky Index with the low irradiance values that are present during the morning and evening.
- Using the new variability terms and analyzing the 1- second data PI screens supported the analysis of others in demonstrating the "smoothing" of power ramps from the irradiance variability even across a small facility such as the Prescott 2.5 MW PV plant. (NOTE: PI is a database collection, storage, and management software produced and sold by OSIsoft®).
- Fast Fourier analysis was valuable in identifying patterns within the time varying power data, allowing for grouping of these events into either regulation or sub-regulation time frames.
- There were a small number of power ramps that induced feeder voltage changes as much as 2% of nominal value.
- While there were a number of power change ramps that were in excess of 7% of PV plant capacity per second, all induced voltage changes were less than 5% of nominal voltage which is well within the regulation requirements of the substation.
- Improvements in ground based weather measurement with satellite data augmentation could improve the quality of forecasting since historical data production data is limited.
- While other methodologies are still being considered for day ahead solar forecasting improvements, MOS forecast provided more value over both day-ahead persistence and GHC (clear sky) for the hourly average energy and over the period of testing.

- There could be value in forecasting variability for generation regulation requirements through an “NVP” (Natural Variability of Power) classification methodology or similar variability ratio analysis.
- Local cloudiness and aerosol conditions complicate any GHI forecasting, and all methods require improvement in the capability to forecast cloud formation, type, speed and direction or localized conditions that affect irradiance reaching the ground.

II. FACILITY AND TEST SETUP

Prescott Airport Solar Facility is an Arizona Public Service owned facility which produces energy and interconnected to the Sturm Ruger substation. While the energy is delivered into the APS system, the original purpose of the facility was to provide APS with experience and data on large scale solar systems as a part of the APS Solar Test and Research (STAR) mission. A variety of types and sizes of PV panels as well as inverters are installed at the facility. Thus, the facility is not a homogenous design; however, the size of the facility provided a good test site for the purposes identified. One issue that arose with the test is that mid-year 2011, the Sturm Ruger substation was modified to accommodate an adjacent, new solar facility and also, several inverters were changed to upgraded models which changed test conditions. Collecting formal test data stopped mid-June, 2011 though all instrumentation remained in place to continue to collect information for future use.

The layout of the facility is shown in Figure 2-1 along with the identification of the locations of test equipment used for this research. Prints were used to determine spatial measurements across the field as necessary to allow for analysis of cloud movement.

For meteorological stations 1 through 4, a variety of instruments were used. The irradiation monitors measured GHI and were LI200X -L15 –PT pyranometers which were selected mainly for their response time, sensitivity, and good temperature range. Response time was important since the irradiation was being recorded every 1-second. Each station also had a wind speed sensor (RM Young Wind Sentry Anemometer) and temperature sensor (107-L). Station 1 also included a Vaisala PTB110 Barometer. Station 5 contained the Yankee Environmental TSP-700 pyranometer which was used as a check on the GHI measurements being taken by the LiCor sensors. Each station sensor was tied into its own CR1000 data logger which in turn was connected to a radio transmitter/ receiver which communicated to a base transmitter/ receiver in the on-site office trailer. This base station was then tied into the APS network to carry the data to a PI server located in Phoenix. Additionally, the network fed each data logger with a time signal to make sure that all information was synchronized. . Also tied into the network was an output from the facility common output Schweitzer SEL351 relay which measured power, voltages, currents, and power factor (VARs). This relay was also synchronized to the APS network time.

All data from the network was directed to and stored on an OSI PI server located in Phoenix with a 1-second resolution. The server was then accessed and data was transferred to data sheets and PI trend sheets loaded into the Renewable Energy server. This data could then be periodically transferred to Northern Arizona University and 3Tier as necessary for additional analysis.

Also located at the on-site office trailer was a Yankee Environmental Services TSI-440A Sky Scanner. This took pictures of the sky at a time increment set by the operator. At first, this setting was every 5 minutes but was changed to every 30 seconds as more data was needed for the analysis. Scanner information were stored locally on a computer and periodically downloaded through the network into an accessible file.

While adjacent to an airport, there was no observed interference or data distortion from air traffic in the area since the flight paths were generally to the south of the facility. In fact, the airport meteorological information was periodically checked to provide verification against the on-site instruments. Also, 3Tier was able to access two weather cameras mounted within the airport boundaries to provide some visual verification of actual weather conditions against the forecast.

To allow for calculations of cloud motion across the facility, the following measurements were taken:

From Station	To Station	Distance (feet)
1	2	948
1	3	1897
1	4	627
2	3	960
2	4	603
3	4	1407
5	1	370
5	2	1308
5	3	2244
5	4	901

From Trailer to End of Field is 2274 ft.
Width at North end is 507 ft.
Diagonal from SW corner to NE corner is 2285 ft.
Facility covers about 25 acres

Table 2-1 Data Station to Data Station Distances

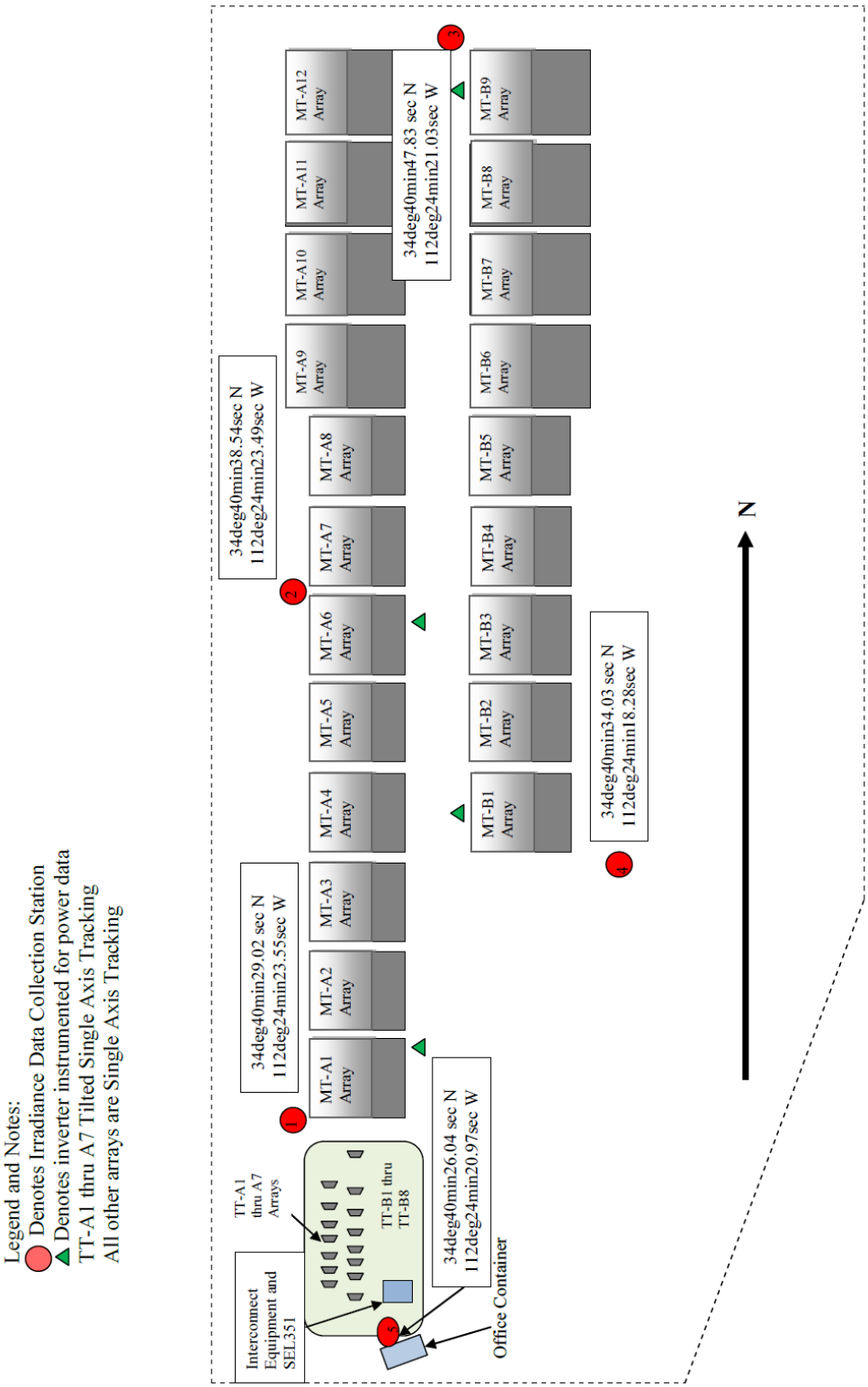

Figure 2-1: Prescott Airport Solar Facility and Instrumentation Station arrangement

III. VARIABILITY

Irradiance Introduction

One of the key purposes for this study was to measure the variations in irradiance and the response of the solar plant power output to these variations. While more accurate measurements of the value of irradiance could have been made with Plane of Array (POA) instruments, Global Horizontal Irradiance (GHI) provided sufficient accuracy of irradiance for the purpose of response comparisons, and since a faster response irradiance sensor was used, certainly provided the trends and data sampling at a rate necessary to provide the analysis desired. This was particularly true since the interest in this study was to look at overall response of a solar facility, not to evaluate the performance of the solar panels or efficiency of the facility. Furthermore, GHI is an output of mesoscale weather models from which solar power forecasts are derived. The facility common power output was measured with an SEL351 with sufficient response to allow for 1-second power and power quality data to be recorded. The challenge that presented itself was how to best analyze and compare the variability seen by both the irradiation and the power output. While data was collected over several months, March, 2011 provided a variety of types of days and was used in much of the variability analysis here. The top graph in Figure 3-1 shows the resource observed at station 1 during the month of March 2011 at a temporal resolution of 1-second. This 1-second dataset was then analyzed to create a time series of the 1-second changes in irradiance and plotted in the bottom graph in Figure 3-1. The top graph shows the expected diurnal variation of solar irradiance with several cloudy or partly cloudy days during the month. It is interesting to note the instances where the irradiance exceeded 1000 W/m^2, which is typically caused by additional radiation collected by the irradiance sensor as the edge of a cloud passes, reflecting additional light onto the sensor (and the PV panels). The bottom plot of the 1-second changes in irradiance shows that the 1-second changes were fairly modest (99% are less than ~50 W/m^2). However, there were instances when the irradiance changes were over 250 W/m^2 per second, which could cause large fluctuations in the PV power output, depending on the nature of the clouds.

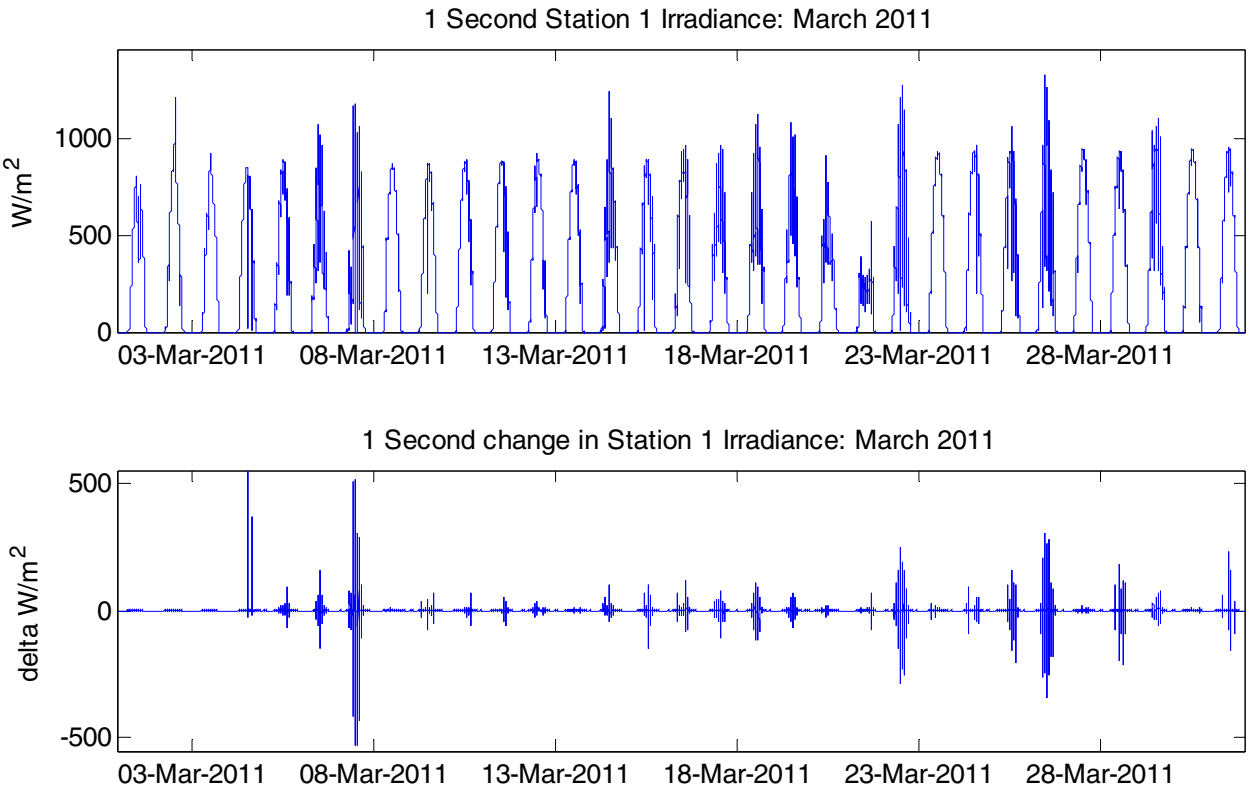

Figure 3-1: Prescott Airport Solar data

Clear Sky Index Analysis

Some techniques used recently to represent variability were presented in a Lawrence Berkeley National Laboratory (LBNL) report by (Mills & Wiser, 2010). One method reported, among others, was to create a "clear-sky index" to characterize fluctuations in irradiance at the site in order to represent the resource variability. This technique of assessing the magnitude of fluctuations in irradiance normalized to an expected clear sky irradiance value has the advantage of creating a "normalized" variability allowing the variability to be compared between different seasons at a given site, or between different sites, etc. Furthermore, it focuses characterization of the variability on the component caused by stochastic cloud processes, and not the changes that occur due to the predictable component of the sun's movement through the sky.

The clear sky index (CSI) is computed as shown below, where $GHI(t)_{actual}$ is the actual global horizontal irradiance measured at time t, and $GHI(t)_{clear\ sky}$ is the global horizontal irradiance one would expect to measure on a clear day at the same time on the same date:

$$\boldsymbol{CSI} = \frac{\boldsymbol{GHI(t)_{actual}}}{\boldsymbol{GHI(t)_{clear\ sky}}} \quad \text{(Eq. 3-1)}$$

Example plots of 1-minute global insolation (which is typically a 1-minute averaged value of the GHI) vs. time and the related 1-minute CSI values vs. time are provided in Figure 3-2.

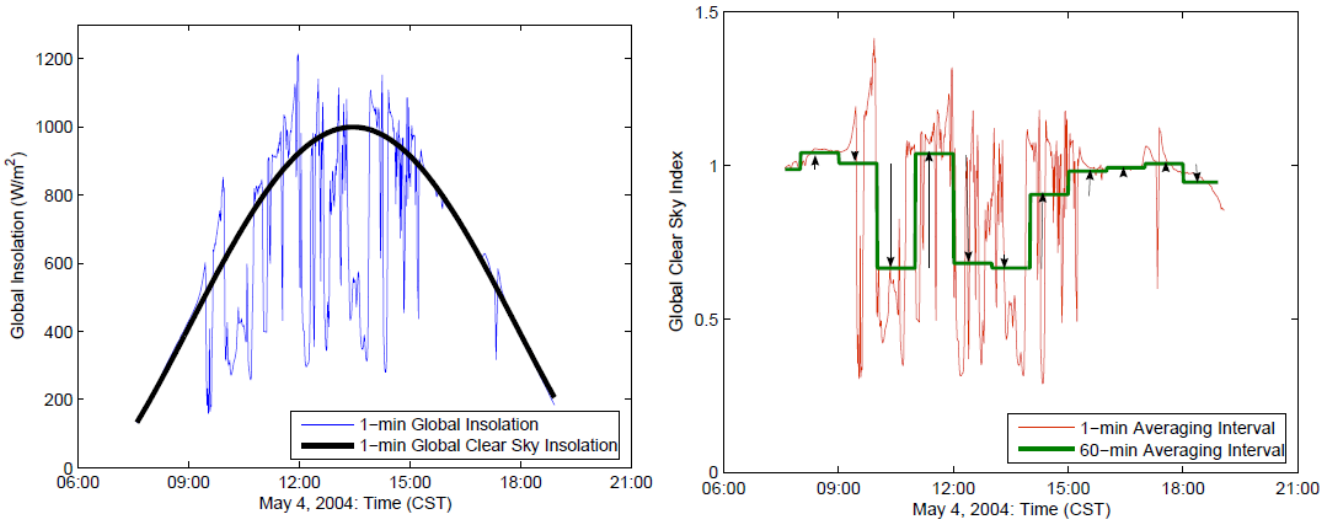

(a) Example of 1-min global insolation and global clear sky insolation on a partly cloudy day

(b) Example of 1-min global clear sky index, 60-min average of the clear sky index, and arrows representing magnitude and direction of 60-min deltas

Figure 3-2: Example plots of the global insolation and associated clear-sky index values; (Mills & Wiser, Lawrence Berkeley Laboratory, 2010)

Two methods to determine the $GHI(t)_{clear\ sky}$ are (1) to perform a theoretical calculation of the GHI based upon the date, location (lat/long), air mass, air transmittance, etc., or (2) to take measurements of the GHI on a clear day. For the purpose of this report, since we have measurements of the GHI on some clear days, it is easiest to simply use these values and compute the CSI of the irradiance for nearby cloudy days. Figure 3-3 shows the one second irradiance (GHI) data measured at station 1 on March 7, 2011, along with the GHI data from March 8, 2011. In order to determine a time series of the clear sky index for March 7, since March 8 was a clear day, its values for the irradiance were used to approximate the clear sky irradiance on March 7. Thus, the CSI values for each second of March 7 can be well approximated with Equation 1 using the GHI values from March 7 in the numerator and the GHI values measured on March 8 in the denominator, producing a 1-second time series of CSI values for March 7. A plot showing a 10-minute time series of CSI values for March 7 is provided on the right side of Figure 3-3. Thus, the plots in Figure 3-3 are analogous to those shown in Figure 3-2, with the exception that 1-second data is used in Figure 3-3 whereas 1-minute data was used in Figure 3-2. It is worth noting that the CSI, while generally less than 1.0 due to the reduction in irradiance by the clouds, does have numerous values above 1.0. These values above 1.0 occur when there are no clouds blocking the irradiance striking the pyranometer, but there are clouds in the vicinity that reflect/refract additional light onto the irradiance sensor. Thus, the irradiance measurement at these moments is actually above the clear sky value and thus the CSI is greater than 1.0. The average value of the CSI for March 7 is 0.318, indicating that the irradiance during any second is, on average, 68.2% less than the clear sky value.

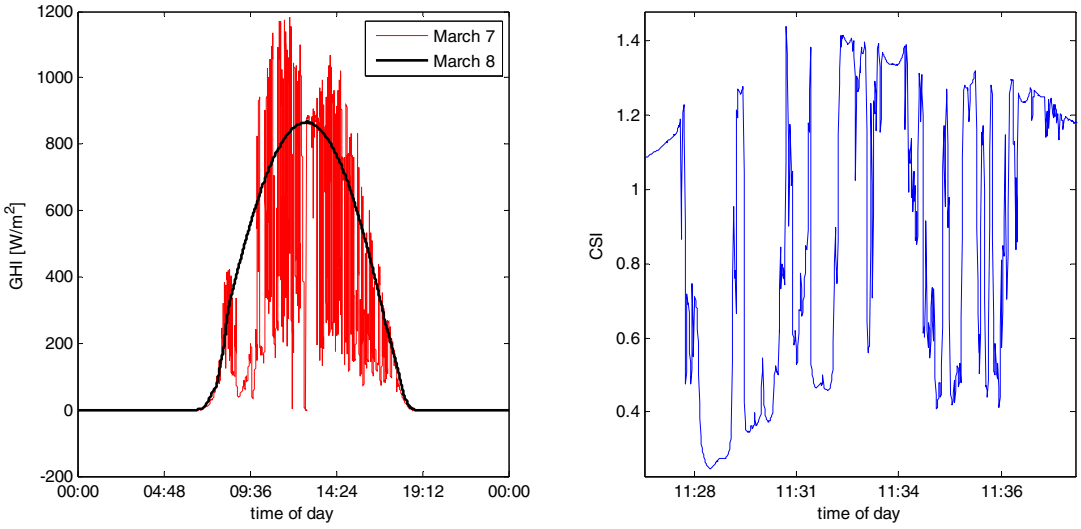

Figure 3-3: Left: The irradiance (GHI) measured at station 1 during a cloudy day (March 7, red line) and during a clear day (March 8, black); Right: The CSI plotted for 10-minutes of March 7, 2011.

Introduction of Additional Analysis Factors

Prior to replicating the work of LBNL or others, some initial thoughts were made concerning how to assign a numerical value to variability. The first, most obvious method was to compute the standard deviation of irradiance, maximum and minimum change in irradiance, and finally the standard deviation of the change in irradiance (other metrics were considered but those mentioned here will help show a chain of thought). Simply taking the standard deviation of the irradiance would remove information about the shape of the data from which it would be difficult to deduce the variability of the data. Identifying the maximum and minimum change in irradiance will aid in identifying the extreme 1-second ramp rates of the irradiance. However, the standard deviation of the change in irradiance is best suited to statistically represent the variability. Normalizing this value about some global value to create a non-dimensional metric aids in allowing direct comparison with the variability during different seasons or months, and even other locations or resources. The following non-dimensional terms were created in order to normalize the data based on a global mean value so they can then be compared easily:
Natural Variability of Irradiance (NVI): Equals the standard deviation of the changes in irradiance from one data point to the next, divided by the mean of irradiance.

$$\boxed{\boldsymbol{NVI} = \frac{\sigma_{\Delta G}}{\bar{G}}} \quad \text{(Eq. 3-2)}$$

Natural Variability of Power (NVP): Equals the standard deviation of the changes in total power from one data point to the next, divided by the mean of the total power.

$$\boxed{\boldsymbol{NVP} = \frac{\sigma_{\Delta P}}{\bar{P}}} \quad \text{(Eq. 3-3)}$$

Natural Variability of Array (NVA): Equals the standard deviation of the changes in array power from one data point to the next, divided by the mean of the array power.

$$\boxed{NVA = \frac{\sigma_{\Delta A}}{\bar{A}}} \quad \text{(Eq. 3-4)}$$

For each of these metrics, the mean value in the denominator uses data from all 24-hours of the day. This was done for ease of calculation, since the number of daylight hours change throughout the period of data collection, using all 24 hours makes it unnecessary to track the sunrise/sunset hours as they change (recognizing the metric would be slightly different and more accurate if only daylight hours were used. Given that each of these metrics is dimensionless, any of the three can be compared directly, simply on the merits of variability across a specific timeframe. All that needs to occur for direct comparison is that the datasets used for irradiance and power have the same timescale (i.e. time increment between data) over the same timeframe (duration of data record).
For instance, if a single value for the month of March is desired for direct comparison, then the variability term (NVI, NVP, or NVA) is simply the standard deviation of the changes in the variable (i.e. irradiance, total power, or array power) between successive data points for the entire month divided by the mean of the variable for the entire month. For example, the NVI based upon the 1-second data for the month of March 2011 would be the standard deviation of the changes in 1-second irradiance (e.g. the standard deviation of the changes plotted in the bottom graph of Figure 3-1) divided by the mean irradiance for the month of March 2011 (e.g. the mean of the 1-second irradiance values plotted in the top graph of Figure 3-1).

If it is of interest to determine how the metric varies per day, then the variability term (NVI, NVP, or NVA) is simply the standard deviation of the changes in the variable between successive data points for a single day of the month divided by the mean of the variable for the entire month. Repeating this computation for each day of the month allows comparison of the variable from day-to-day. If it becomes desirable to determine how the metric varies per hour, then the variability term is simply the standard deviation of the changes in the variable between successive data points for a single hour of the month divided by the mean of the variable for the entire month; repeating this calculation for each hour of the month.

NOTE: The variables used in the calculation of each of the standard deviation values NVI, NVP and NVA are specific to the Prescott Airport solar facility. However, a discussion concerning the mean values used in the denominator of these terms (NVI, NVP, NVA) suggested that these values could be more universally applied by selecting a common power and irradiance reference comparison of these terms between completely different sites. For example, the NVP denominator in this analysis was the average power output since this facility was difficult to characterize whereas a facility specifically designed for power operation could easily substitute the nameplate capacity. For NVI, rather than use long term average irradiance in the denominator, a common value of 1000 W/m^2 could be substituted and would be recommended for a more universal application and ability to compare between facilities. ("Comments on presentation materials from Dave Willy", Joshua Stein, Sandia National Laboratories, May, 10, 2011.) Either way is most likely acceptable depending on application, but it should be made clear of the term that is used in the denominator.

What Provides the Best Frequency of Data Collection

The plot in Figure 3-4a was derived to help better evaluate the question of what frequency of data collection is necessary to correctly characterize the variability and ramps in power production. The two upper lines in this figure show the absolute value of the maximum change in power between two successive data points recorded on March 7 and March 10, plotted vs. skip step, and referring to the left-hand axis. Note: Skip step is a simulation of changing the periodicity between samples of data collection; it is the change in time between two successive data points over which the maximum change in power is measured. As displayed in Figure 3-4a, on March 7, which was a cloudy day (top blue line in plot), the maximum change in output increases from about 210 kW between successive 1-second data points (i.e. a skip step of 1) to in excess of 75% of the full March 7 plant capacity of 2200 MW for data points separated by 30-seconds (i.e. skip step of 30). For data points separated by 15-seconds, the max change in power was 1490 kW, or about 65% of the plant maximum capacity. Note for the green curve shown, corresponding to the sunny day of March 10, that the absolute value of the maximum change in output between successive data points varied from about 30 kW for 1-second data to 300 kW for 30-second data points, or roughly 1/6 of the magnitude of changes experience on cloudy March 7.

Next, Figure 3-4a also shows the rate of change of the power calculated by dividing the maximum change in output by the time interval of the corresponding skip step interval. For example, at a skip step of one, dividing the absolute value of the maximum change in power (210 kW) by one second, the rate of change of power is found to be 210 kW/sec. Repeating this calculation for all values of the skip step produces the red curve (March 7) and the turquoise curve (March 10). The scale for these lines on the right axis was deliberately set to be the same as the left axis in order to show it in relationship to the magnitude of the maximum change. However, it is useful to enlarge the scale to get a better view of the rates of change, so these exact two lines are plotted in Figure 3-4b, except that the scale on the left axis is enlarged.

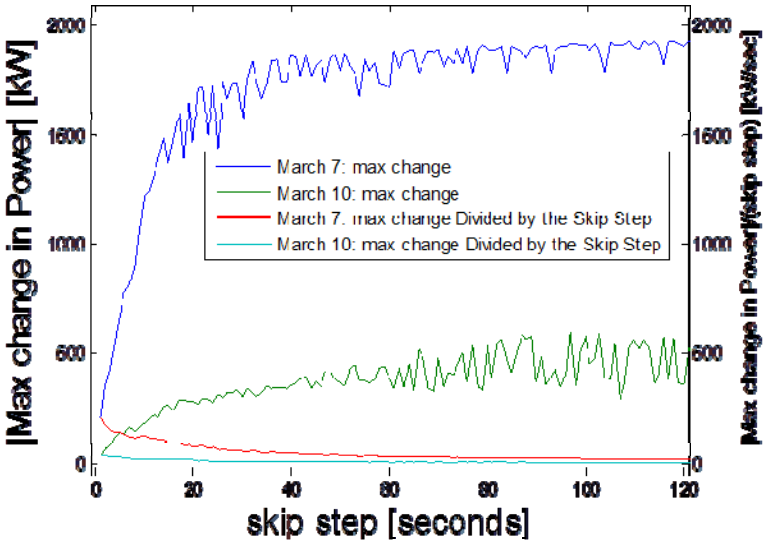

Fig. 3-4a: Skip Step Method Max Change in Power and Rate of Change of Power

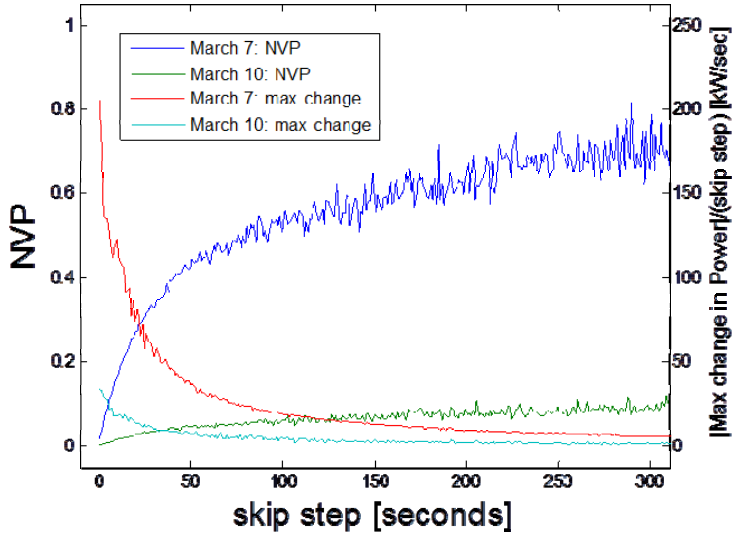

Fig. 3-4b: Skip Step Method Results (3-4a) expanded, left axis expanded

As can be seen, cloudy March 7 represented by the red line has a peak rate of change for the 1-second data, rapidly falling off as the time interval between successive data points is increased (210 kW/sec for 1-second data, 170 kW/sec for 2-second data, 150kW/sec for 3-second data, etc.). Thus from this testing at least, 1-second data or better provides a much better understanding of the maximum rate of change of power at the PV plant. However, 4 to 5 second data may be sufficient to evaluate changes in output that exceed some specified magnitude, for example 500 kW. However, it is clear that for this size of power plant, there is considerable variability in the output occurring in the 1-second time frame or less.

Referring back to Figure 3-4b, the leveling off of the NVP curves over 30 to 300 seconds suggests that ramp rates may have reached their maximum values before these time frames. (For more information on PV ramp rates, see the "Regulation, Sub-regulation, and Ramp Rates" Section IV). Also note the difference between the traces shown in Figure 3-4b for days 7 and 10, which demonstrate the NVP values for a relatively cloudy and a relatively clear day, respectively. The March 10 trace (clear day) shows the NVP value due to the predictable movement of the sun across the sky, and not due to cloud-driven variability. An advantage in determining the NVP values for the power plant, as opposed to a clear sky index, is that it is easily translated into an actual "average" change in power, which is useful when concerned about variations on the transmission or distribution line. To demonstrate this point, using the lines plotted in Figures 3-4a and b, the average power output for the month (using all 24 hours of data from each day) was 0.642 MW. Thus if the NVP is equal to 0.7 for a time step between data points of 240 seconds (4 minutes) on March 7, then the average value of the changes in output between successive data points four minutes apart is 0.7 multiplied by 0.642, equal to 0.45 MW, etc.

For comparison, the same "skip step" analysis was performed using the clear sky index for March 7, 2011. Figures 3-5a and b show that a similar result can be generated whether using the change in irradiance or the change in CSI. Calculating the changes in CSI over time from the data used to generate Figure 3-3 for March 7 is plotted in Figure 3-5a, and a plot of the maximum (absolute value) changes in CSI vs. skip step intervals, in other words the "CSI deltas", yields the chart shown as Figure 3-5b. This plot is comparable to the NVP curves in Figure 3-4b (the differences noted in the figure will be discussed shortly).

.

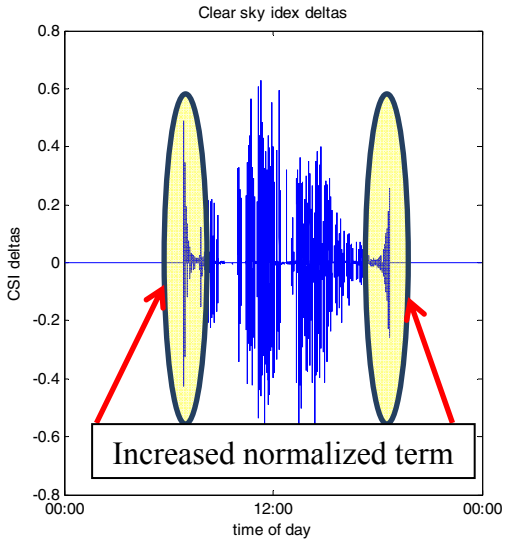

Figure 3-5a: Changes in CSI over time using Figure 3-3 Data

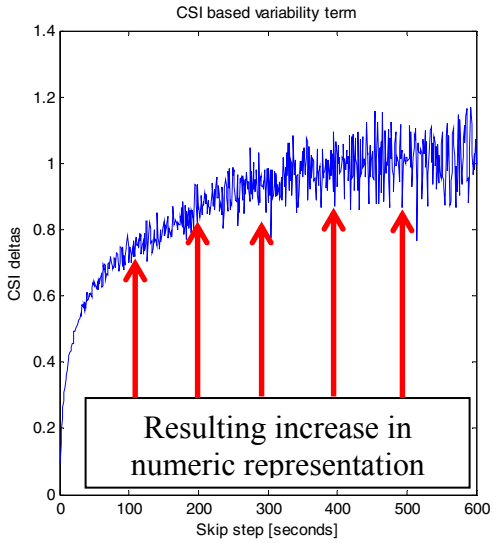

Figure 3-5b: Maximum changes in CSI using skip step method

Another important question to investigate is the necessity to acquire instantaneous power and irradiance data or if collecting time-averaged data is sufficient. To address this, the NVP computed using the instantaneous power data is plotted in Figure 3-6 (upper blue line, "skipping data"; the same plot as in Figure 3-4b) along with the NVP computed using the time-averaged data (lower red line, "average data"). To compute the NVP computed using time-averaged data, instead of skipping data points as was done for the blue line, all of the data collected during the time interval was averaged. For example, at an interval of 100-seconds on the abscissa of Figure 3-6, successive data points in the power time series were created by averaging the previous 100 data points. Next, the NVP was computed using this time series of averaged power data points. As is evident by comparing the two curves shown in the figure, the variability reported is substantially reduced when time-averaging the data.

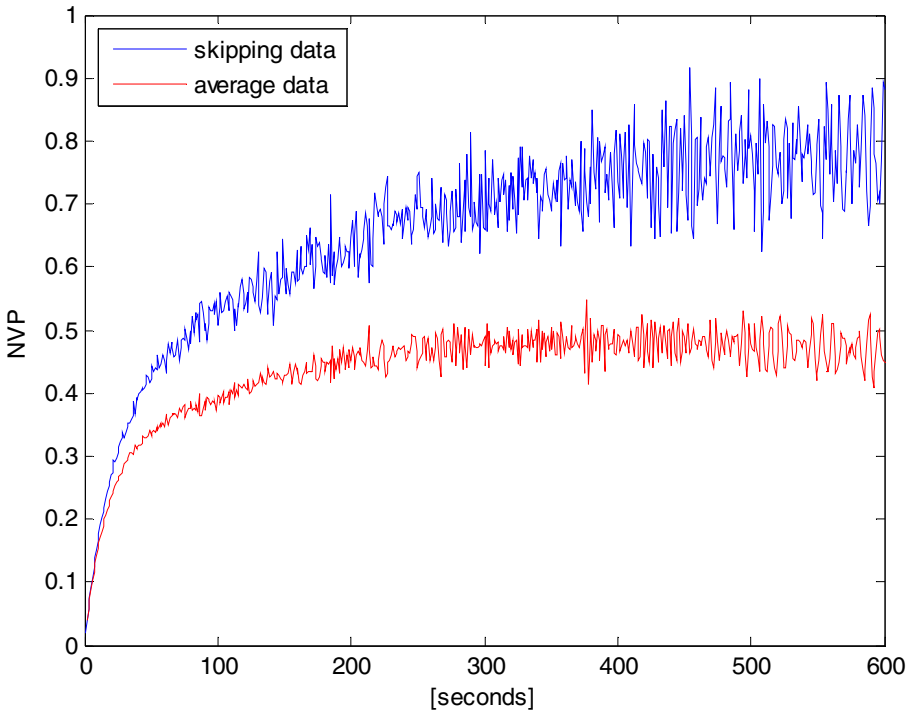

Figure 3-6: Variability in the power data across different time intervals observed in the data by skipping data (actual changes) versus averaging data

The preceding analyses showed that the closer to obtaining one second data, the better the characteristic of the variability and, in particularly, the rates of change of power that could be described. This is not intended to imply that 1-second data must always be used. Indeed, it would depend on the needs and accuracy required of the analyses; however, it has been demonstrated that any periodicity beyond about 30 seconds creates a significant loss in the capability to understand the variability.

Additional Observations from NVI/ NVP and the CSI comparisons

Some additional interesting observations can be made with Figure 3-5a and b. Note the actual irradiance data for March 7 plotted from the PI system as shown in Figure 3-7. While there was some modest amount of variability in the irradiance present in both the morning and late afternoon in this data, note that in 3-5a, this magnitude of variability is greatly enhanced as indicated by changes in CSI. Since CSI is computed as a fraction using a perfect clear day irradiance at that particular time of the day in the denominator, (so a low number in the morning and evening) and the actual irradiance in the numerator), the fraction becomes large in the early morning and late afternoon hours even though the actual changes in the irradiance are not very large. Thus any changes in irradiance will be seen as a much larger percentage of change in the numerator yielding larger changes in CSI Index. (NOTE: For this reason, the Mills and Wiser, 2010 report excluded the times near sunrise and sunset. For further clarification, per Mills, the data were limited to times when the cosine of the solar zenith exceeded 0.15 (i.e. the sun had to be at least 9 degrees (approx.) above the horizon.) While less prevalent during the mid hours of the day, this phenomena appeared to be present throughout the day as indicated by Figure 3-5b having maximum changes in CSI larger than seen by the corresponding curve of maximum changes in NVI seen in Figure 3-4b. In other words, for highly variable days and the morning and late afternoon hours, this comparison would suggest that using the CSI method tends to indicate higher variability than that actually present, and although less prevalent during the middle of the day as variability peaks become greater, a larger variability is represented by the CSI method than may actually be present. However, the method used should be determined by that method that best serves the purpose. The LBNL study was interested in the correlation of changes in output due to the distance between clouds. For this purpose, CSI method removes the impact of the sun from any of the variability metrics whereas the NVP method would not. On the other hand, this study was primarily focused on measuring overall variability and its effects on power regulation, voltage regulation, and ramping, and the NVP method provided a good method for this purpose.

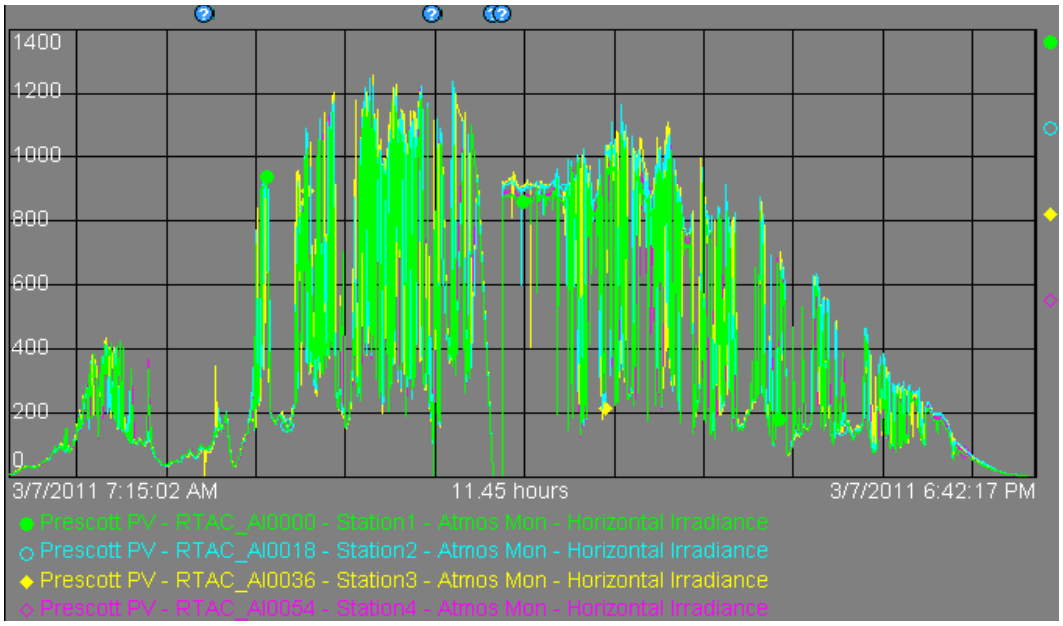

Figure 3-7: March 7 Irradiance Data

Reduction of power output variability across distance or "smoothing":

There have been several studies which discussed the fact that spatial diversity of facilities will smooth the variability presented to the grid. One such study was conducted by Lawrence Berkeley Laboratory in 2010[3]. The study collected data from multiple sites as far away as 450 km from each other and found that even with a highly variable day, the spatial diversity acts to average out the variability seen at each site with the variability from the other sites. Thus, the average across all the sites will be much reduced as seen in Figure 3-8.

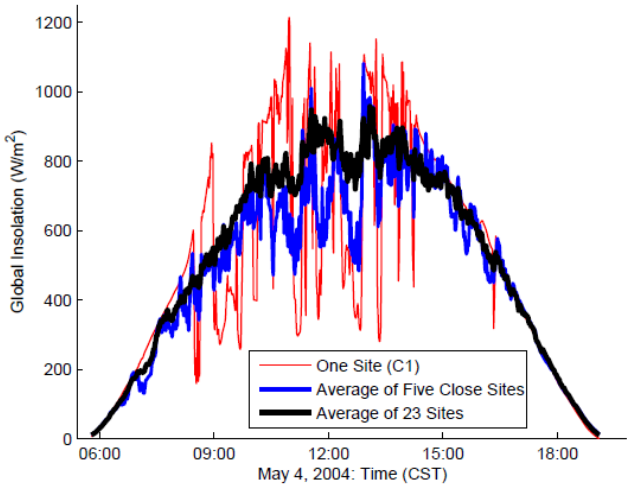

Figure 3-8: Plot of averaging irradiance measurements from nearby sites (Mills& Wiser, Lawrence Berkeley Laboratory, 2010)

In this study, however, there was more of an interest in determining if even smaller spatial distance will provide a dampening or smoothing effect on the irradiance variability to the total power variability. The variability terms NVI and NVP can also be used to observe the smoothing in fluctuations that occurs across the solar facility. In this research the pyranometer at each station was used as an in situ irradiance measurement whose output was considered in determining the variability at a single point in space. The power output of the entire power plant was measured in relation to the variability of irradiance integrated across the entire special domain of the facility. Figure 3-9 shows the variability computed for each day of March for the irradiance observed at station 1 (NVI), the average of the irradiance at stations 1-4 (NVI), and the variability in the power output of the power plant (NVP). As shown, the variability of the power output (the NVP) was noticeably lower than the NVI of the irradiance from station 1, and also less than the NVI based upon the average irradiance measured at stations 1-4. This figure provides an initial indication of the spatial smoothing in the irradiance fluctuations that occurs as the effective size of the measurement area increases which essentially integrates the irradiance over a larger area.

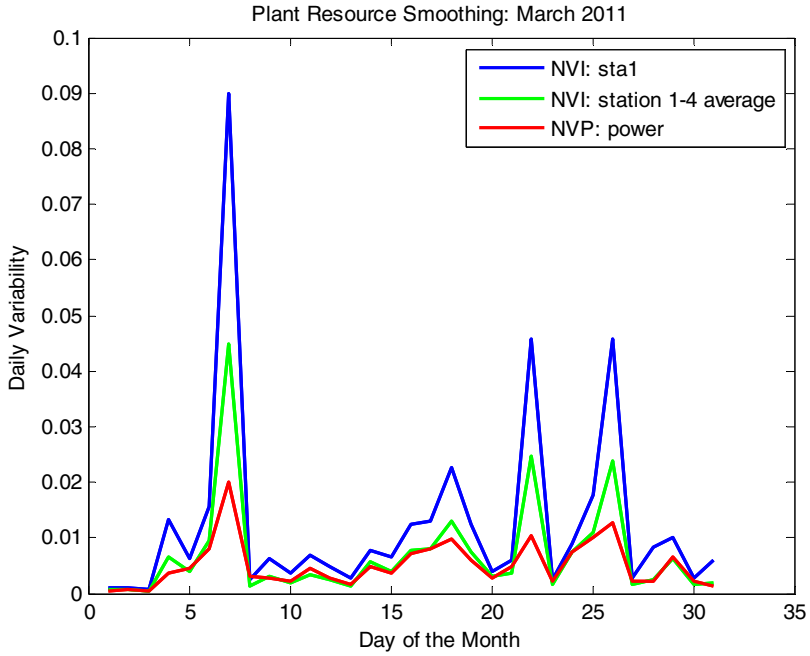

Figure 3-9: Daily NVI and NVP calculations based upon 1-second changes in irradiance and power: March 2011.

Also shown in Figure 3-9 was the fact that the NVI computed by averaging the irradiance from four pyranometers placed around the perimeter of the power plant was quite a bit greater than the NVP. Thus, an average irradiance from four stations or even more will not accurately portray the variability in power output on cloudy days. This can be due to many factors such as direction and change of direction of the cloud passage, speed of the cloud movement, opacity of the clouds, and potentially other items related to the

individual layout and response of the facility, but mainly, however, this is due to the spatial distancing between the irradiance measurements and the size of the facility.

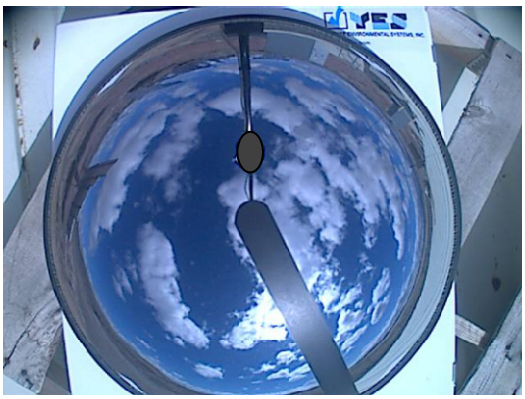

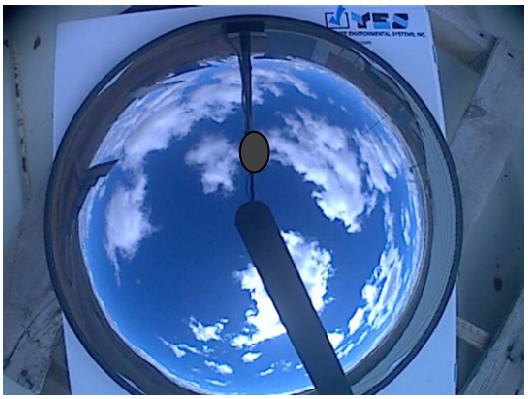

1135 am 1140 am

Figure 3-10: Cloud activity on March 7 at times specified

Note: Top of picture is due north

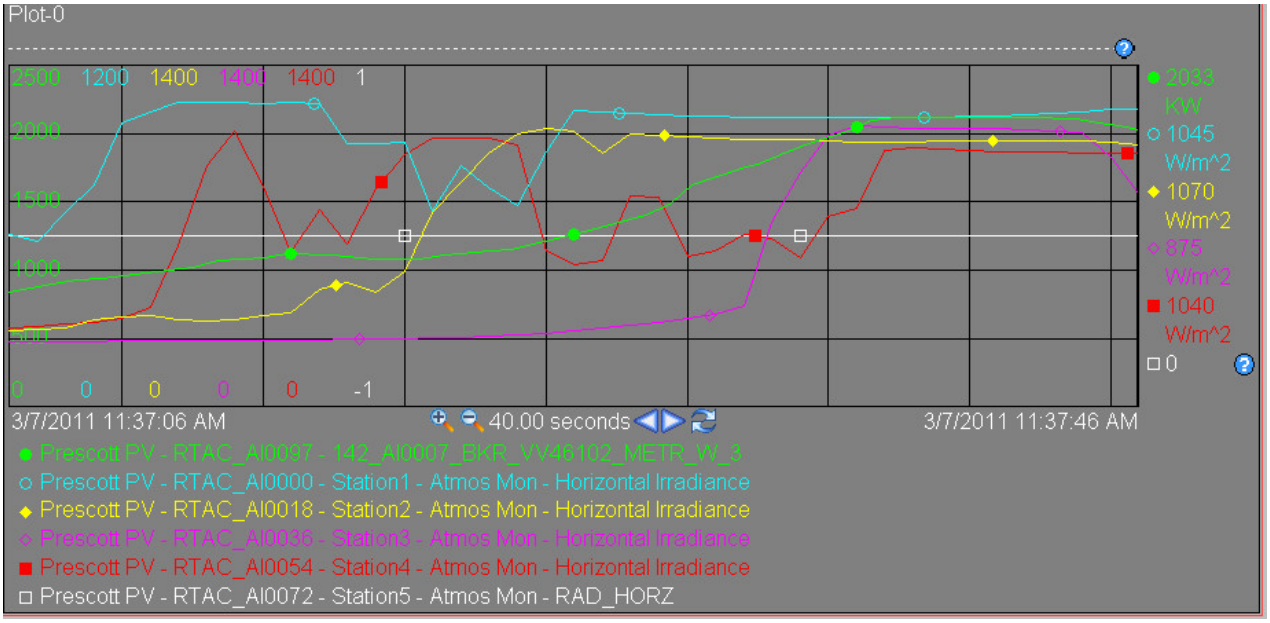

Figure 3-11: PI Data for March 7 over 40 second period showing cloud related power rise

This smoothing analysis was also supported by data observation. Figure 3-10 shows the cloud activity over the Prescott facility on March 7 between 1135 and 1140 while Figure 3-11 is a PI graph of the 1-second data in a 40 second period during this time. Notice in Figure 3-10 that, in general, the day was a pleasant, sunny day with scattered cumulus clouds, but the data in Figure 3-11 and Figure 3-9 indicates that this was the highest variability day for the month of March. At the beginning of the trend, the facility was operating at some reduced power output due to cloud cover. As the cloud moved across from southwest to northeast, more sections of the PV field were uncovered as seen by the

trends on the irradiance stations. Station 1 began to trend upward at 11:37:06 with Station 4 beginning at 11:37:10. While the irradiance at these monitoring stations on the edges of the PV field rose fairly quickly (spike upward), the Common Output (green line) began a trend upward at a much slower pace. Station 2 began its rise at 11:37:19 but at a much slower pace with Station 3 at the far north end of the array starting at 11:37:32 very quickly. While the most rapid rise in irradiance was less than 4 seconds, Common Output rose from about 850 kW to about 2100 kW in 32 seconds or 1.86 %/second. In other words, the transit time from Station 1 at one end of the field to Station 3 at the other end of the solar field was 26 seconds, an equivalent cloud speed of 50 miles per hour, yet even with a small array as Prescott, the distance across this field acted to reduce the ramp effects of the irradiance on the overall output of the facility.

This observation example of the irradiation vs. power output supports the NVI/ NVP analysis of Figure 3-9; that is, even as concentrated as this solar facility was, there was generally sufficient distance from one end to the other to smooth out or dampen the sharp effects of irradiation ramps caused by cloud movement. Obviously, this would be highly dependent on the plant layout with respect to the predominant weather patterns in the location of the power plant. This means that development of a plant power curve alone may not be sufficient. In the selection of the location and design of large solar facilities with power output variability imposed on the grid a concern, consideration may need to be given to how any given area of the facility may be more concentrated in panels with respect to other areas. This could result in power ramp rates that differ and are more or less steep across the overall power ramp curve than a more homogenous layout of the facility. More shall be discussed on this point in Section IV as variability is related to ramp rates and system needs to counteract this variability.

Summary of Variability Discussion

In this section, new terms, NVI, NVP, and NVA were introduced to help describe the variability of both irradiance and of the power output from a field. The denominator in these terms was used in a manner specific to the Prescott Airport Solar facility. While the denominator could use data specific to a given facility as was done, it would be fairly easy and recommended to use a more general value in the denominator to allow a more general use between differing facilities. These variability terms have been used in exploring observed irradiation and power data to propose several findings.

- First, the shorter the time interval for the data collection, the more accurate the ramp characteristics of the variability will be. The analysis would indicate that the closer to 1-second data collection that can be achieved, the more accurate the analysis of the variability. Longer periods, such as 2, 3, or even 10 seconds can also be useful, but the closer the data collection period approaches 30 seconds, the less accurate the variability analysis will be.
- Averaging, even with short interval data, results in minimizing key information on the nature of the peaks of the variability and can result in misrepresenting the

true impact of the variability of the irradiance on the output of the facility. This is another reason that shorter intervals will provide a much clearer picture of the variability.

- The NVI/ NVP methodology may provide improvement in analysis of the higher levels of variability over the clear sky index analysis particularly in the morning and evening periods when average irradiance and power output have much steeper ramps.
- Using the NVI/ NVP terms and the evaluation of 1-second recorded data supports the conclusions and work of others that, even with a smaller facility, the distance from one end of the field to the other will limit or smooth power output ramps even with large and fast peaks in irradiance.

IV: VARIABILITY EFFECTS ON FACILITY OUTPUT

Discussion

While understanding the variability of the irradiance is important, the effects of the irradiance on the output and what effect the total facility output might have to the grid or distribution line to which it is connected is the purpose of this study. The rating of the solar facility was about 2.5 MW maximum and the substation to which it was connected was 10.5 MVA resulting in about a 24% penetration, yet no significant voltage transients were experienced even for the most dramatic ramp rates. This shall be discussed in the text below. The discussion here will also provide basis for analysis technique for further planned studies by APS.

Questions arise concerning how the facility power output variability will affect the power grid or substation; that is, will the variations in load net solar power output be in the regulation time frame (and thus handled by regulating units on the transmission grid) or the sub-regulation time frames(and therefore handled locally on the distribution feeder), or both? Under ideal conditions, the facility power increases and decreases output with the changes in sun angle throughout the day and donates the energy to the transmission system through the distribution it is connected, and the system generation only needs to respond to balance these energy changes to the system in a fairly smooth manner. However, clouds and aerosols introduce variability to the energy changes which must be compensated. Low frequency variability generally will result in a mismatch between the energy provided between the generation and the energy required by the load. The generation responds by increasing or decreasing to meet this variation through a process called regulation. The system typically consists of several generators which are on Automatic Generation Control (AGC) that will respond very quickly to both load variability and the solar variability. In some instances, there can be localized mismatch between the load and the solar output as well as impedance changes with decreasing solar to the point that the substation corrections must occur through tap changers or switched capacitors. In this paper, tracking minute-to-minute fluctuations is referred to as regulation. However, as seen in the variability section, significant power ramps can occur within seconds, and these variations that are less than a minute are called sub-regulation here. For higher frequency variability (sub-regulation) caused by the solar facility, the loads being fed from the substation can be affected with variations in voltage without some compensation. In most instances, the solar facility inverters will compensate for these changes in the sub-minute periods and/or the transfer of energy between substation and the transmission is sufficient to assure sufficient energy is supplied to match load needs; however, if the variability gets significant with large scale penetrations compared to the feeder size, other measures must be considered to assure that the quality of the power (voltage and frequency) remains within limitations set by the utility and governing agencies. This could mean requiring installation of controls at the solar facility interconnect such as a quick acting variable reactance devices which would act to “filter out” these variations before reaching the substation. Or the utility could

decide the solar facility or aggregated solar generation on the substation is too large and place limits on the amount of solar generation interconnecting to the distribution system. In some instances, some utilities have made decisions to terminate the variable generation to avoid the power quality issues.

Fourier Analysis

To better understand the periodicity of the power output fluctuations present in the data obtained from Prescott, a Fourier analysis was performed using the Fast Fourier Transform. The basic idea behind a Fourier analysis is that any continuous, time-varying signal, such as the power output from the Prescott solar site, can be represented by a combination of harmonics of sine waves of different amplitudes and frequencies. One advantage in performing such an analysis is that it allows one to identify patterns in a time-varying signal that may be of importance, but not obvious from looking at the time series data itself. For the study of the PV power output variability, it was desirable to identify time-varying components of the output power with frequencies within the load following (10-minutes to an hour), regulation (1-minute to 10 minute), and sub-regulation (< 1 minute) time frames. These would be the frequencies of signal variation that will impact load following units on the transmission system, regulating units on the transmission system, and regulation actions at the transformer and the signal quality on a distribution line.

To determine the frequency content of a discretely sampled time-varying signal (e.g. the power output), a Discrete Fourier Transform can be utilized. A Fast Fourier Transform (FFT) is a computational approach to solving a Discrete Fourier Transform. Applying an FFT to a discretely sampled, time-varying signal will result in a representation of the signal by a combination of multiple sine waves of varying amplitudes and frequencies. It was used in this study to identify the magnitude of resource variability over different time periods that will also be present in the power output, and could therefore potentially affect the transmission system. FFT's are typically displayed in a "frequency spectrum", such as that shown in Figure 4-1b for the irradiance measurements recorded at Station 1. This particular figure shows the "% of total signal", which refers to the percent of the overall signal amplitude due to variations at a given frequency or period, plotted on the vertical axis versus "Period" on the horizontal axis. The plot on the upper half of Figure 4-1b shows the period in hours, up to 25, and the plot on the lower half focuses in on the waves with a period of less than 70 minutes, with the period displayed in minutes. These frequency spectrums were created using the 1-second data observed at Station 1 on the relatively clear day, March 8, 2011 whose plot of irradiance vs. time is shown in Figure 4-1a. As expected, most of the total signal was composed of a two periods: 24hrs and 12hrs, corresponding to frequencies of 1 and 2 cycles per day, respectively. Note the vertical scale in the plot on the lower half of Figure 4-1b is of order 10^{-4} (0.0007% max), so there was essentially no energy in these lower period high frequency variations. Two dominating modes with little content in the other frequencies would be expected on such a sunny day, due to the obvious diurnal variation of the sun's radiation, and the irradiance signal appeared as a single bump on a sine wave. Periods of 6 hrs or less that showed local peaks on the frequency spectrum plot (though at a very small magnitude)

corresponded to other harmonics of the base frequency of 24 hrs (1/2 = 12 hrs, 1/3 = 8 hrs, 1/4 = 6 hrs, …, 1/24 = 1 hr, etc.).

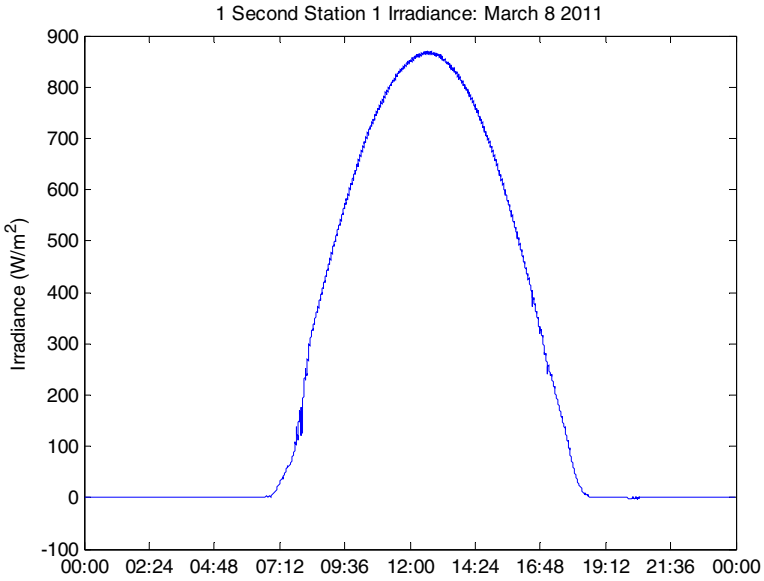

Figure 4-1a: March 8, 2011 Irradiance vs. time

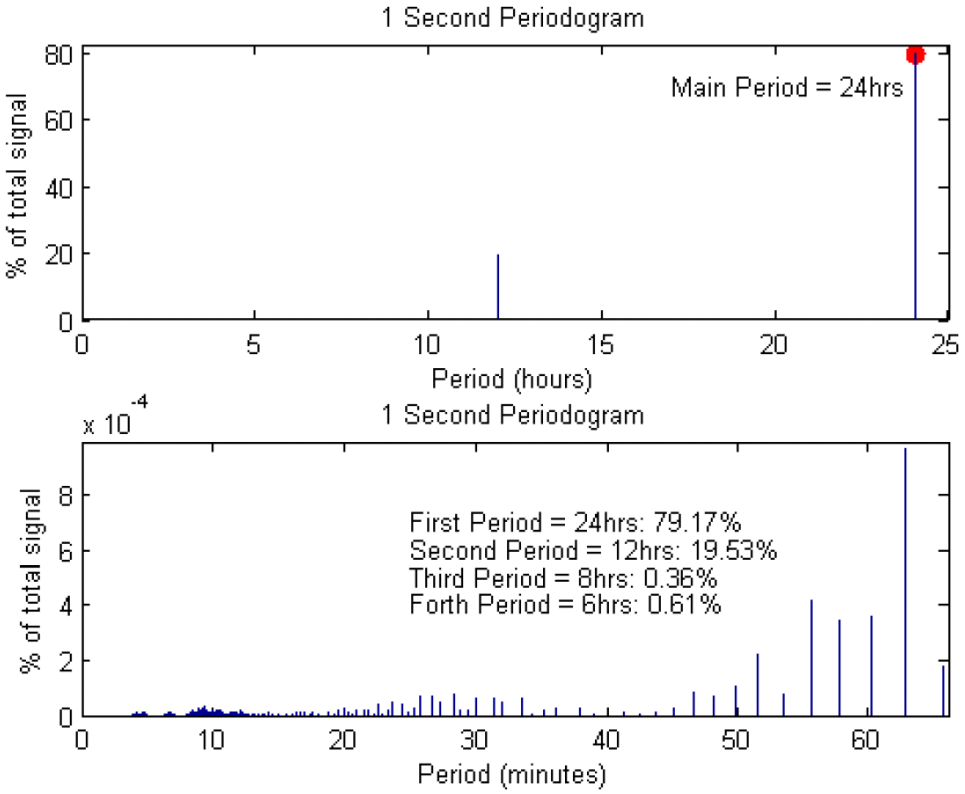

Figure 4-1b: FFT of a sample clear sky day, March 8, 2011

A significant difference was observed in analyzing the FFT of a partially cloudy day, in this case the same March 7, 2011 day, as used in the Variability section of this report. For convenience, the 1-second irradiance data for March 7 that was plotted in Figure 3-3 is plotted again in Figure 4-2a, and the results of the FFT for this data plotted in Figure 4-2b. When comparing the frequency spectrum in these plots to those in Figure 4-1b, note the scale on the vertical-axis in the upper plot is slightly lower, and that of the lower plot is four orders of magnitude larger than that shown in Figure 4-1b. Thus the shorter periods (higher frequencies) contributed a much larger fraction to the amplitude of the signal. Also indicated was the related decrease of signal percentage of the primary periods (24 and 12 hrs/cycle), and peaks in the shorter period variations (higher frequency) were seen at several points on the frequency spectrum, with periods near (in minutes/cycle) 2, 6, 8, 10, 13, 16, 20, 25, 30, 45, and 60. These were relevant because the first two (2 min/cycle and 6 min/cycle) are in the time frame of regulation on the transmission grid, while the remaining frequencies transition from regulation to firmly within the load following time frame. It can be inferred from this plot that there would be regular occurrences in the regulation and load following time frames due to solar variations. Also note that as the period approaches 1 second data collection frequency, the highest temporal resolution recorded for this study, the "density" of periods observed increased (typical for an FFT).

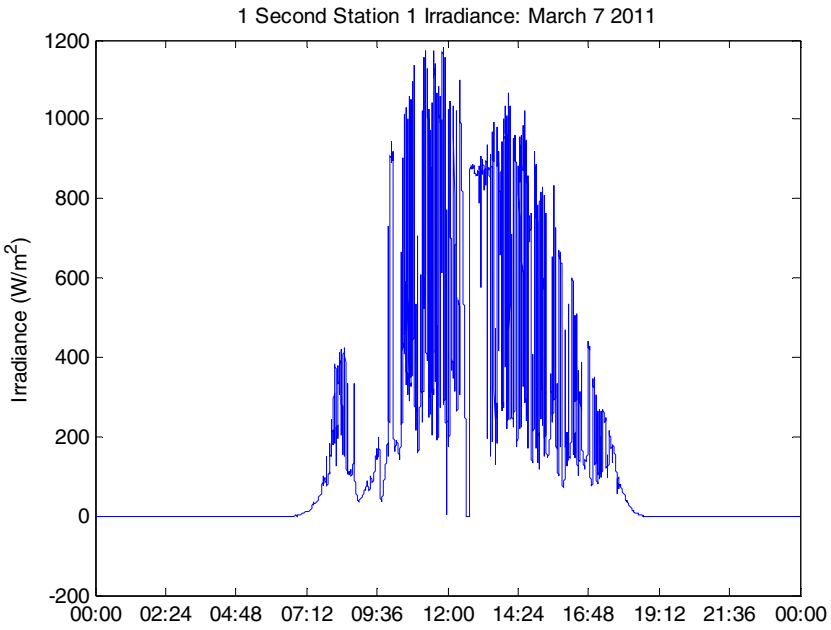

Figure 4-2a: March 7, 2011 Irradiance vs. time

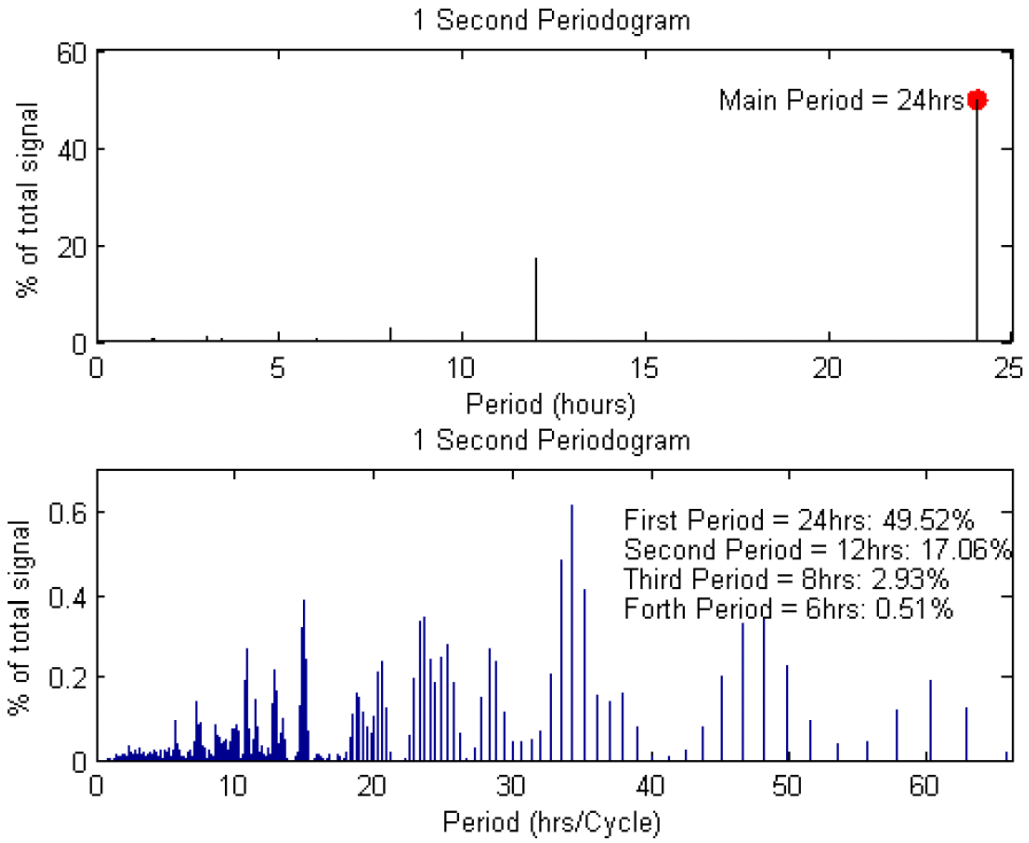

Figure 4-2b: FFT of a sample cloudy sky day, March 7, 2011

The FFT analysis was performed in this study with the intent of identifying frequencies observed within the temporal resolution recorded in the regulation and load following time frames, and frequency content was observed in the 1-second irradiance time-series data within the load following, regulation, and sub-regulation time frames. While not necessarily unexpected, the analysis provided a much better understanding of the need to further analyze the occurrence of these events. Wavelet analysis was not performed here. While wavelets would provide a much better understanding of the characteristics of the individual events, the interest in this study focused on the frequency of events and effects of those events.

Regulation and Sub-Regulation

The first task in tabulating the variations in the regulation and sub-regulation time frames is to define a method to break down the power signal measured at the PV power plant in the appropriate time frames. Figure 4-3 shows about 3.5 minutes of the 1-second resolution power data collected at the Prescott power plant (the total power output of the plant). The black line represents the 1-second power data, the red line connects

successive 1-minute mean power data points, and the blue line connects successive 10-minute mean power data points (only one of these points is shown). The blue line that represents the more gradual 10-minute change in production would combine with the remaining net load and be dealt with by the load following units on the transmission grid. The "regulation" data points are defined by determining the difference in the 1-minute mean data point and the 10-minute mean line, as shown in the plot:

$$\boxed{\boldsymbol{R = PS - PR_t}} \quad \text{(Eq. 4-1)}$$

where: R = regulation data point
PS = 1-minute mean value of power
PR_t = linearly interpolated 10-minute mean value of power

Thus, one regulation data point is defined for every 1-minute averaged power production data point. These 1-minute variations in the average power output, when combined with remaining 1-minute averages in the load to form a net load, are handled by the combined generation on the transmission system tasked with regulation. The "sub-regulation" data points are defined, one for every 1-second data point collected, by taking the difference between the 1-second data and the 1-minute mean line, as shown in Figure 4-3:

$$\boxed{\boldsymbol{R_{sub} = P_t - PS_t}} \quad \text{(Eq. 4-2)}$$

where: R_{sub} = sub-regulation data point
P_t = instantaneous 1-second power data point at time *t*
PS_t = linearly interpolated 1-minute mean value at time *t*

These variations must be controlled through energy transferred into the distribution substation or interconnect transformer system to assure that proper voltage levels are maintained within specifications. If the voltage deviates from specifications, other methods such as tap changers, energy storage or other power quality devices must be employed.

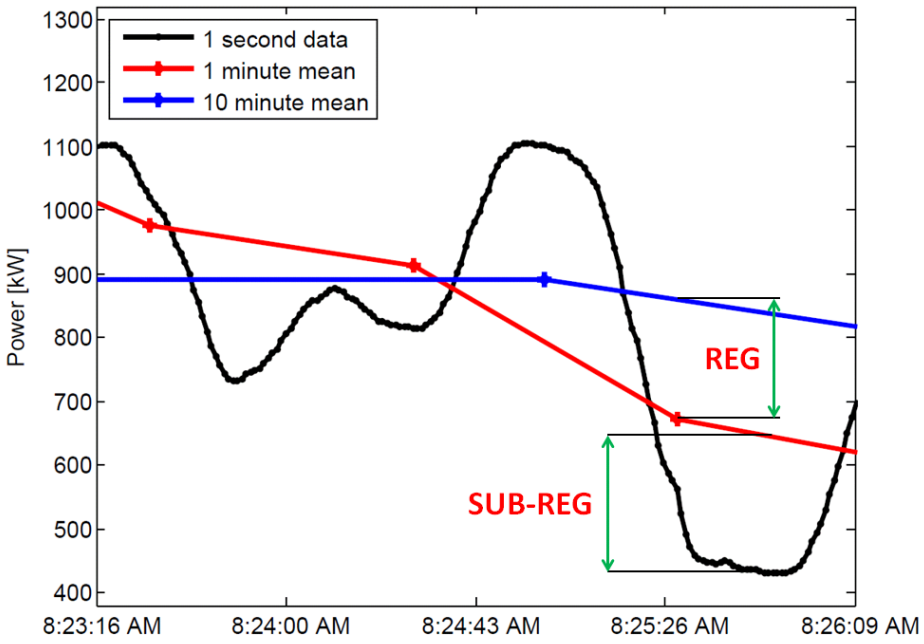

Figure 4-3: A plot showing how regulation and sub-regulation data points are determined

This method was applied to separate the regulation and sub-regulation signals from the overall power output time series for, once again, the cloudy day March 7, 2011 and resulted in the time series of regulation and sub-regulation signals as presented in Figure 4-4. Note the large magnitude of both the regulation and sub-regulation changes that resulted in power output.

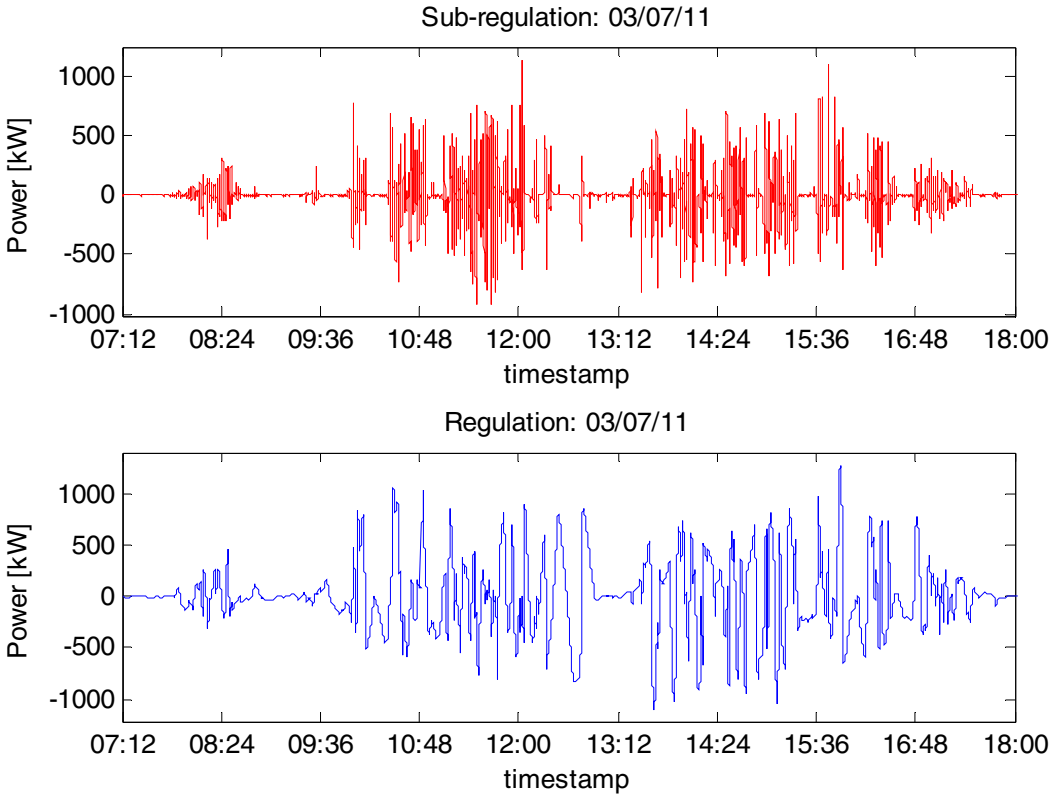

Figure 4-4: Example time-series of sub-regulation (left plot) and regulation signals (right plot)

Histograms tabulating the regulation and sub-regulation values determined for the same day are provided in Figure 4-5. Once again note the large magnitude of some of the regulation and sub-regulation signals indicate potential effects on the distribution line power quality that may need some type of compensation.

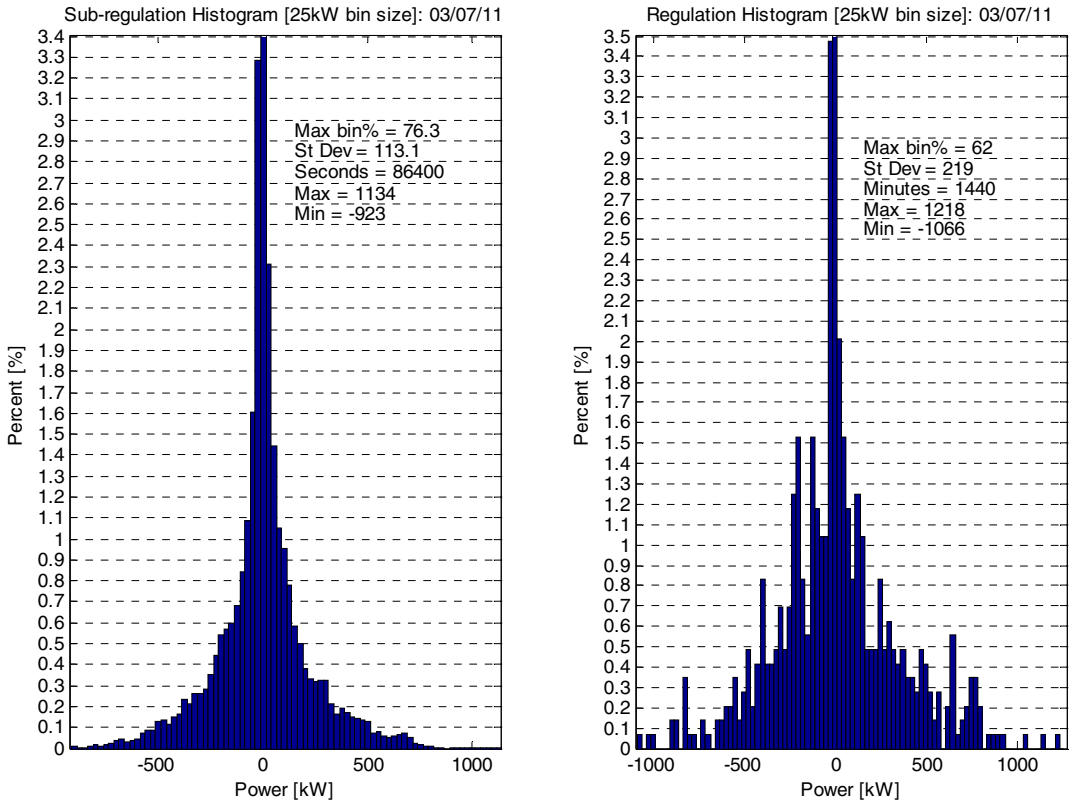

Figure 4-5: Histogram of resulting requirements of sub-regulation (left) and regulation (right) for March 7, 2011

Similar histograms created for all the regulation and sub-regulation values for February, March, and April 2011 are shown in Figures 4-6 and 4-7. A summary of key statistical results for these months are presented in Table 1, which shows the standard deviation, minimum, maximum, 95.5%, 99.0%, 99.7%, and 99.9% values. The first two rows of the table present the statistics for relatively cloudy and clear days, respectively, followed by the results for each month and all three months combined. The histograms shown in Figures 4-5, 4-6 and 4-7 demonstrated that the distribution of 1-second fluctuations observed at the Prescott site are not Gaussian (normal), but had a much higher peak in the center of the distribution. This means that the majority of the regulation and sub-regulation requirements were very small. The histograms also show that there were some, though relatively few, 1-second changes that were quite large (>500KW). As shown by the red, dashed line on the left side of Figure 4-5, 99.7% of the sub-regulation 1-second changes during the three month period were less than 296 kW. This result is also displayed on the bottom-right side of Table 4-1, which also shows that 99.95 of the 1-second fluctuations were less than 445 kW. This implies that 0.1% of the 1-second fluctuations (about 7,690 over the 3-month period) exceeded changes of 445kW (either up or down).

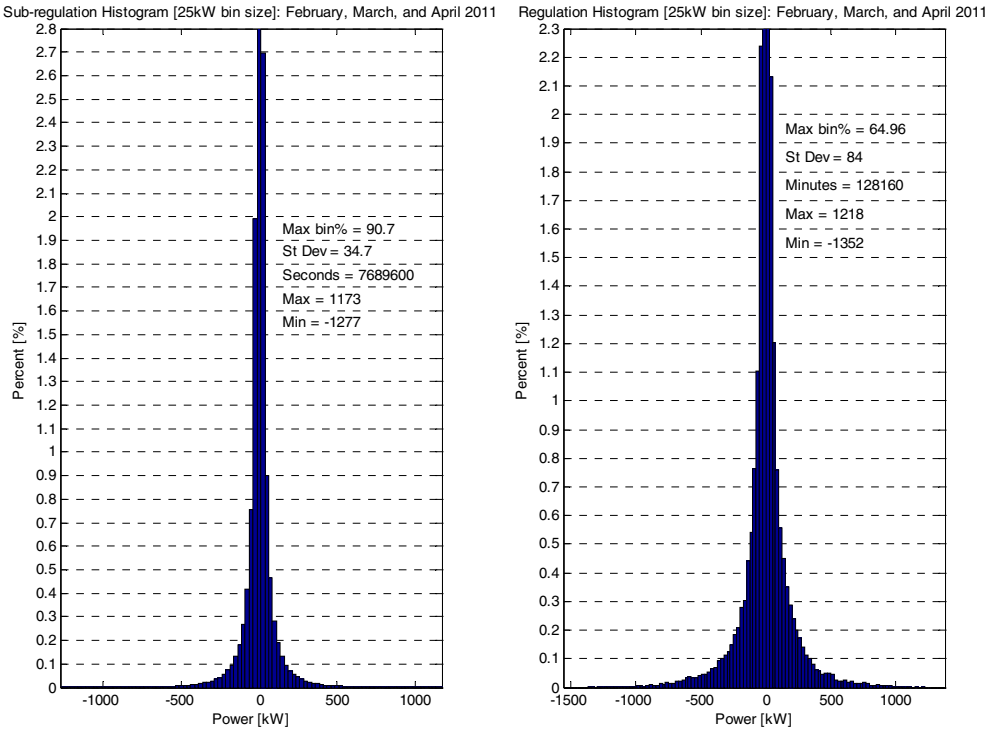

Figure 4-6: Histograms of 1-second subregulation (left) and 1-minute regulation (right) values
March, April, and May 2011

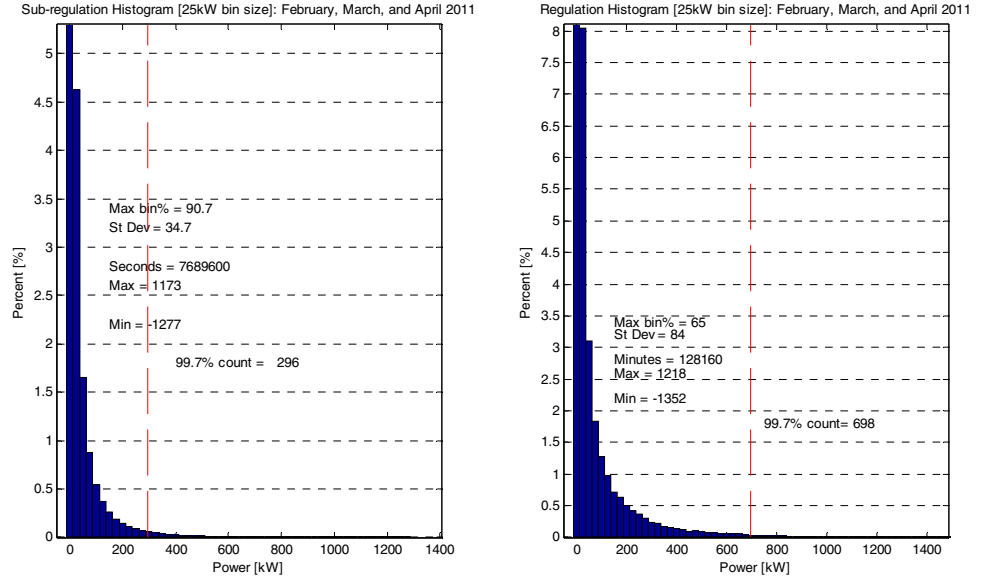

Figure 4-7: Histograms of the absolute values of 1-second subregulation (left) and 1-minute regulation (right) values
March, April, and May 2011

		σ (kW)	Min (kW)	Max (kW)	95.5% (kW)	99.0% (kW)	99.7% (kW)	99.9% (kW)
3/7/2011: relatively cloudy	Reg	219	-1066	1218	606	853	1027	1096
	Subreg	113	-923	1134	287	540	689	794
3/8/2011: relatively clear	Reg	8.6	-89.3	79.7	15.3	39.7	66.7	79.2
	Subreg	3.6	-67.2	34.9	8.1	15.4	21.7	27.3
February	Reg	67.7	-1195	1090	120	352	557	771
	Subreg	29.0	-1118	832	28.8	128	254	379
March	Reg	90.5	-1275	1218	180	470	731	917
	Subreg	35.4	-1030	1134	46.5	160	295	452
April	Reg	90.5	-1352	1125	162	495	752	949
	Subreg	38.5	-1277	1173	40.4	172	332	497
February, March, and April	Reg	84.0	-1352	1218	155	438	698	901
	Subreg	34.7	-1277	1173	39.0	154	296	445

Table 4-1: Some key results pertaining to the regulation and sub-regulation signals tabulated February, March, and April 2011

Ramp Rates and Ramp Events

The regulation and sub-regulation statistics indicate the frequency and magnitude of power fluctuations from the Prescott PV solar facility; however, they do not provide any information about the rate at which these fluctuations occur. A ramp rate is defined simply as the rate at which power fluctuates over time:

$$\boldsymbol{ramp\ rate} = \frac{\Delta \boldsymbol{P}}{\Delta \boldsymbol{T}} \text{ (Eq. 4-3);}$$

where, ΔP is the change in power over time period ΔT.
Defining a ramp rate event, however, is not a simple equation, and some method must be arrived at to determine the starting and ending point of a ramp, and thus the magnitude of power change and duration of the ramp.

Three methods were considered: the piecewise linearization "arc-chord" method, the "swinging door" method (sometimes called the "swinging window"), and the "dead-band" compression method [(Horst & Beichl, 1996)[4], (Makarov, Loutan, Ma, & de Mello, MAY 2009)[5], and (EVSystems)[6]]. The "arc-chord" method measures the arc of the data and the direct chord length between points, and using a maximum threshold value declares a ramp event when the difference between the arc and the chord exceeds the threshold value. The "swinging door" method uses a vertical tolerance or error band to create a parallelogram for the data to fit within and is frequently used in data compression. If a data point lies outside of the parallelogram, the previous point is considered the "turning point" between two ramps, see Figure 4-8.

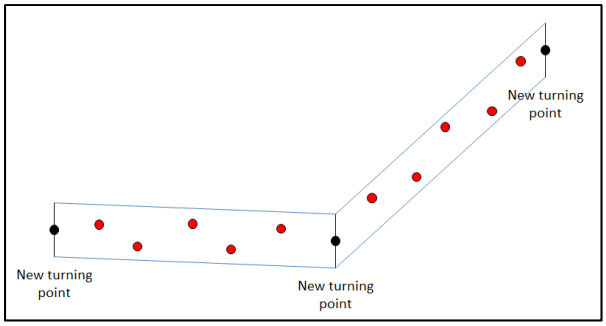

Figure 4-8: "Swinging door" data compression method

Another data compression method is the "dead band" method where error bands are used to create high and low angle tolerances for the following data point. The "swinging door" and "dead band" methods are similar to each other in their results, but it was found that the "dead band" compression method was easier to implement. Since the "dead band" algorithm doesn't need to look back in time like the "swinging door" method does, the "dead band" method is consequently faster. As a consequence, the "dead band" method is the preferred method for use in this study.

In order to catch all ramps that are occurring, the "dead band" method is applied as demonstrated in Figures 4-9 and 4-10. To perform this method in a forward looking, time-preserving fashion, an aperture window is created for each error band used. These aperture windows, shown in Figure 4-10, have a high and low angle as bounds created by drawing a line between the last turning point and the bounds of the error band of the last point. Next a line is drawn between the last turning point and the new point. If the angle of the new point is outside the bounds, then the previous point is the new turning point. If the angle is within the bounds, then the process continues to the next point. As the process continues, the angles bounding the critical aperture tighten based off of the lowest high-angle and highest low-angle of the process, until a turning point is identified. Once a turning point is identified, the aperture angles are reset, the points between the turning points are removed, and the process continues to the next data point.

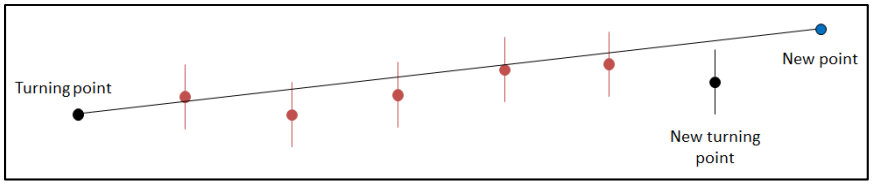

Figure 4-9: The "dead band" data compression method

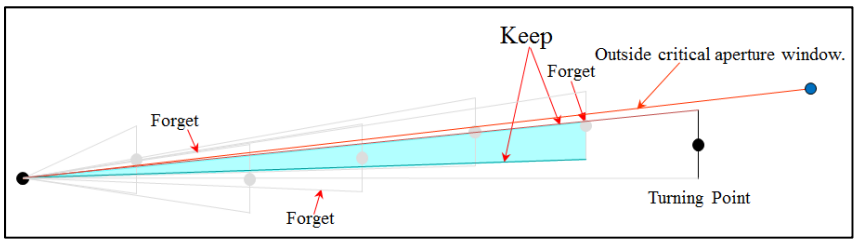

Figure 4-10: Aperture windows created to identify turning points

The dead band algorithm was performed using an error band equal to 5% of the 2.5 MW nameplate capacity of the plant. This value was selected through trial and error, by visually identifying that the ramps identified by the algorithm appeared to fit the data well. This value of 5% may be different for other PV power plants, depending on site specific variability and plant size, but is adequate for this analysis. Thus, the error band is equal to 125 kW (62.5 kW above and below the data point). As displayed in Figures 4-11 and 4-12, which shows the underlying 1-second data and the ramps that were identified, the "dead-band" method appears to capture the actual ramps observed.

It is worth noting here that these methods, as applies, identify many short ramps, many more than would be realized by regulating or load following units on the transmission system, but that may be felt in the sub-regulation time frame and on the distribution feeder.

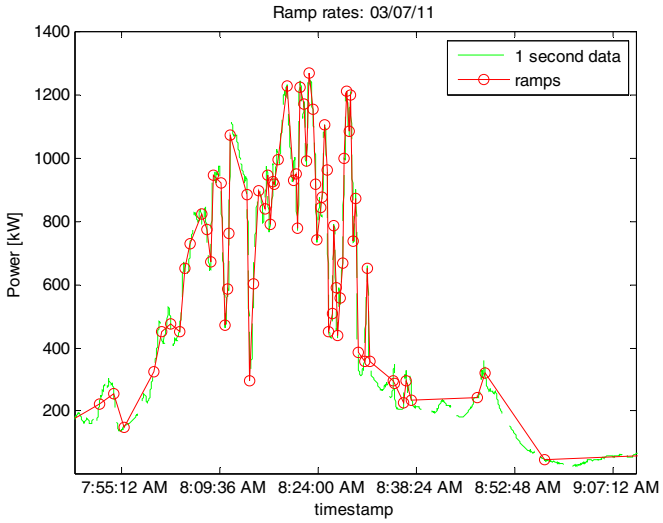

Figure 4-11: Example of ramps identified using the "dead band" method
(Each ramp begins and ends with an open circle, and is connected by the solid red line)

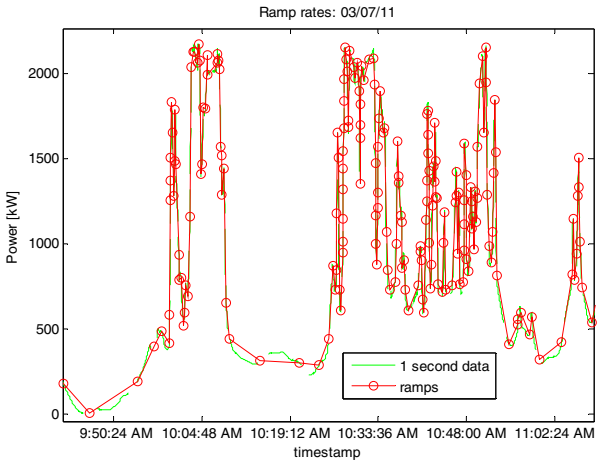

Figure 4-12: Another example of ramps identified using the "dead band" method

In evaluating what regulation and sub-regulation actions are necessary to respond to the variations in PV output, providing a method for determining ramps and ramp rates is important to learn more about the characteristics of typical ramps and also identifying worst case ramps and ramp rates. While the variations directly affect the PV plant output, the concern really is how much the variations carry forward to the overall interconnect point for affect on the "net load" at the feeder, in this case, with the substation. Since substations also carry loads, "net load" is the interaction of the PV variability with the variability of the connected loads, and the total substation voltages must remain within the required tolerances to maintain customer power quality which shall be discussed later. To maintain the quality, the substation must interact with the high voltage transmission system supported by generation and also provide independent power quality control, so it is important that the variations experienced from the solar facility are within the capability of the substation design to maintain the system requirements. Otherwise, changes to the distribution system or the PV feeder must be made to provide the additional compensation.

The dead band method of identifying ramps was applied to data collected for February, March, and April 2011. The resulting histogram of ramps for the entire period is shown in Figure 4-14, while Figure 4-13 shows a histogram tabulating the ramps that occurred on March 7, 2011 (a cloudy day). A summary of the important numerical results is shown in Table 4-2. As demonstrated in the histograms, the dead band algorithm (as implemented with the 5% error band) identifies primarily short duration (< 1 min) ramps, some of which are of large magnitude. The longer duration ramps identified are typically over periods when there is not a large change in output. For the values in Table 4-2, it is important to know that the values were generated for the magnitude and ramps and ramp rate by using the absolute value of the data (thus not distinguishing between down ramps and up ramps). This was done because of the relatively similar distribution of positive and negative ramp events (even though a few negative ramps far exceeded the positive ramps). As presented in Table 4-2, the average duration of the ramps identified over the three-month period of March, April and May was 147 seconds, the average of the absolute value of the magnitude was 171 kW, and the average of the absolute value of the ramp rate was 13 kW/sec. Furthermore, 99.7% of the of the absolute value of the ramp rates were less than 163 kW/sec, and the maximum ramp rates identified were -417 kW/sec (down ramp) and +231 kW/sec (up ramp). In Table 4-2, in the cells that indicate the maximum duration of the ramps, note that the maximum ramp duration is very long on the order of 27,000 seconds (~7.5 hours). This is due to the output of the power plant being limited to 2.5 MW by the power inverters, and that in turn causing the power output to be clipped across the middle of the day on relatively sunny days[1]. This in turn creates one very long shallow ramp across the middle of the day.

[1]The power rating of the panels (~3 MW) exceeds the power output rating of the inverters (~2.5 MW).

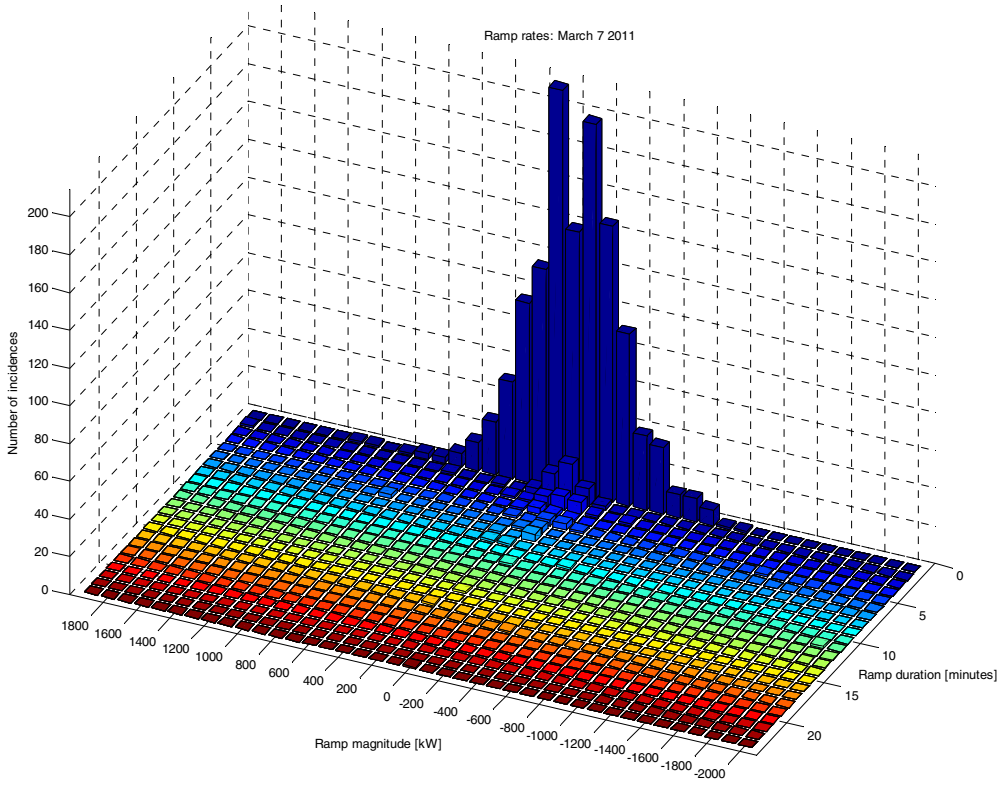

Figure 4-13: A histogram of ramp rates using the "dead band" method for March 7, 2011 (a cloudy day)

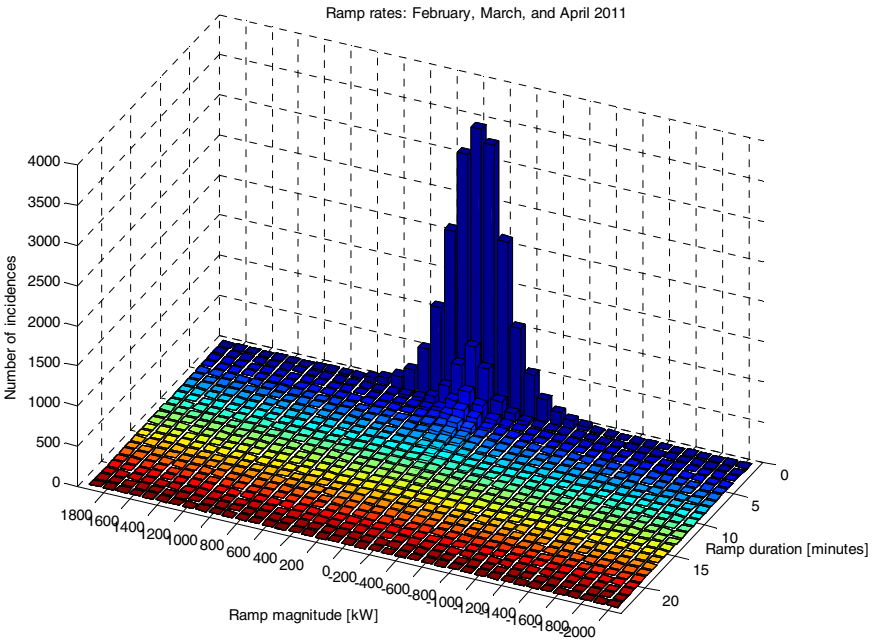

Figure 4-14: A histogram of ramps identified using the "dead band" method for the months of March, April and May 2011

NOTE: Colors for Figures 4-13 and 4-14 are only used to distinguish between ramp durations

		units	σ	ave	Min	Max	95.50%	99.00%	99.70%	99.90%
3/7/2011: relatively cloudy	duration	seconds	101	30.0	1	1949	119	371	832	1510
	magnitude	kW	285	213	-1941	1876	579	819	1171	1876
	ramp rate	kW/sec	53.7	35.5	-186	206	132	161	179	186
3/8/2011: relatively clear	duration	seconds	2259	1759	59	9564	5431	9564	9564	9564
	magnitude	kW	247	179	-561	624	561	624	624	624
	ramp rate	kW/sec	0.46	0.33	-1.19	0.99	0.99	1.19	1.19	1.19
February	duration	seconds	780	163	1	27551	621	2722	6519	10954
	magnitude	kW	240	170	-1604	2064	496	788	1185	1481
	ramp rate	kW/sec	22.6	11.5	-201	191	49	108	142	167
March	duration	seconds	521	128	1	13102	527	2339	4145	7531
	magnitude	kW	233	166	-1941	1876	477	758	1020	1731
	ramp rate	kW/sec	25.2	12.0	-222	206	53.286	126	156	179
April	duration	seconds	906	158	1	28263	525	2478	6044	12456
	magnitude	kW	245	177	-1400	1436	527	791	1076	1260
	ramp rate	kW/sec	31.7	15.3	-417	231	71.4	148	178	196
February, March, and April	duration	seconds	739	147	1	28263	558	2489	5431	10170
	magnitude	kW	239	171	-1941	2064	500	779	1082	1380
	ramp rate	kW/sec	27.0	13.0	-417	231	57.7	132	163	186

Table 4-2:
A summary of important numerical results pertaining to ramps tabulated for the months of March, April, and May 2011

Ramp Rates in the "Sub-Regulation" Time Series

In the previous section of this report sub-regulation was defined as the difference between the 1-second output in power minus the 1-second interpolated values of the 1-minute mean (see Figure 4-3, solid red line). By defining sub-regulation this way, sub-regulation ramps can be defined using the dead band method and the sub-regulation time-series of data points. Identifying ramps in this way should eliminate the portions of the ramps that will be handled by regulation or load following units on the high-voltage

transmission system and not "double count" them as part of fluctuations that will have an impact locally on the transmission distribution line. Figure 4-15 shows an example of ramps identified using the sub-regulation time-series data ramps identified using the dead band method, with the bands equal to 50 kW (2% of the nameplate capacity). This value was selected for the dead band because it appeared to track the ramps, as confirmed by visual inspection of the data (as shown in Figure 4-15). Note that the method identifies the ramp events and preserves the sharpness of the ramp edges.

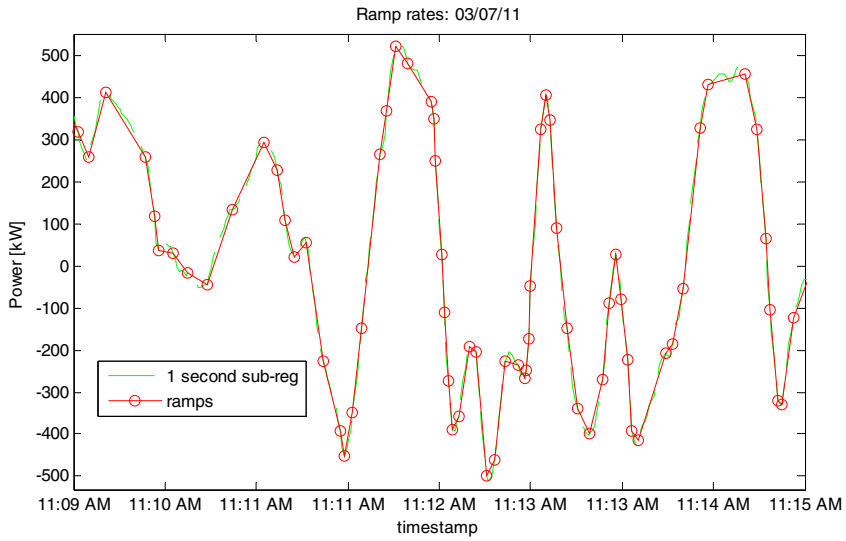

4-15: Example of ramp events observed in the sub-regulation time series data

Figure 4-16 shows histograms of the resulting duration, magnitude, and ramp rates for the ramp events identified during the months of February, March, and April 2011. Notice, from the top left plot of Figure 4-16, the bulk of the ramps identified are between 1-30 seconds in duration. The top right plot in Figure 4-16 shows that the magnitude of most ramps is between -500 to 500 kW, and the bottom plot shows the preponderance of ramp rates occur between -50 to 50 kW/s.

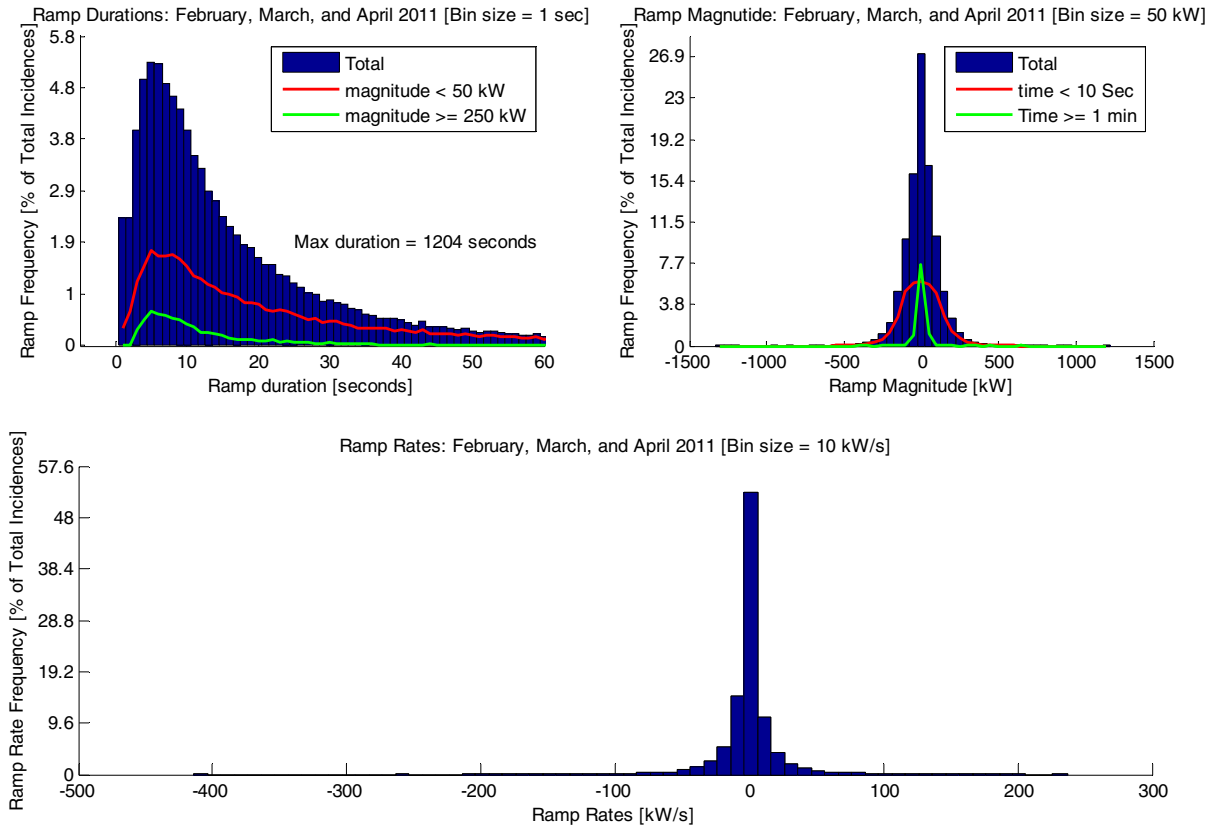

Figure 4-16: Histograms of ramp events observed in the sub-regulation time series data

The resulting ramp events observed in the sub-regulation time-series data can also be viewed in Figures 4-17 and 4-18, and Table 4-3. Figure 4-17 can be interpreted by identifying the color outlining the number of incidences for the corresponding ramp duration and magnitude. For example, the darkest blue, outer line equals 100 incidences and the dark blue line within that indicates 200 incidences. Between the lines can be interpreted approximately linearly between 100-200 incidences. Figure 4-17 shows a peak in the ramp events with duration of approximately 6 seconds, with most ramps of magnitude ±100kW. The underlying data used to create the contour plot in Figure 4-17 is provided as a reference in Table 4-3.

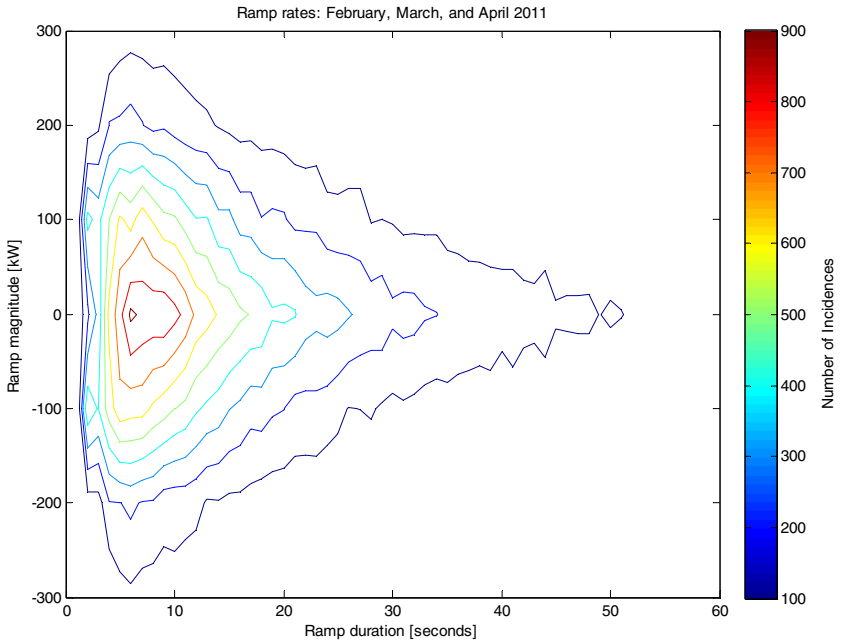

Figure 4-17: Contour plot of Ramp events observed in the sub-regulation time-series data

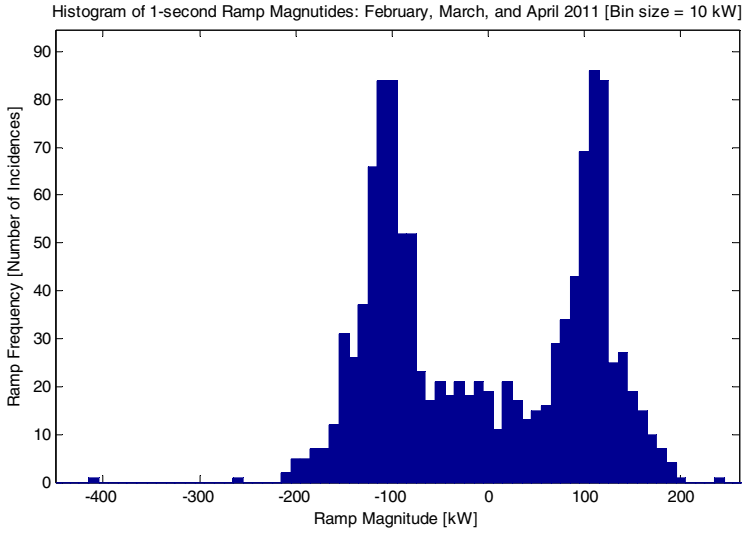

Fig. 4-18: Histogram of 1-second ramp magnitudes observed in the sub-regulation time-series data

An interesting aspect of the data displayed in Figure 4-17 (and Table 4-3) is that there were a significant number of 1-second ramp events. Figure 4-18 shows a histogram of all ramp magnitudes that occurred at 1-second duration. In looking closely at the dark blue line (outer line) of Figure 4-17 (and the underlying data in Table 4-3), there are a significant number of large changes in power magnitude (150 kW or greater); however the greatest majority of these were of duration (5 to 20 seconds). In looking at the ramp duration of 1-second, the left hand side of the Figure 4-18, the ramp rate is 417 kW in 1-

second or 417 kW/sec but with a maximum change in the power of the facility of about 17%. Also looking at Table 4-3, the largest power change seen for a ramp event (disregarding a complete shutdown of the facility) was about 1350 kW but it lasted over 22 seconds for a ramp rate of 61 kW/sec.

Ramp Duration [Seconds]	Ramp Magnitude [kW]																										
	-1350 -1250	-1250 -1150	-1150 -1050	-1050 -950	-950 -850	-850 -750	-750 -650	-650 -550	-550 -450	-450 -350	-350 -250	-250 -150	-150 -50	-50 50	50 150	150 250	250 350	350 450	450 550	550 650	650 750	750 850	850 950	950 1050	1050 1150	1150 1250
1	0	0	0	0	0	0	0	0	0	1	1	53	473	173	428	48	0	0	0	0	0	0	0	0	0	0	0
2	0	0	0	0	0	0	0	0	0	0	0	63	395	333	366	81	0	0	0	0	0	0	0	0	0	0	0
3	0	0	0	0	0	0	0	0	0	0	5	193	550	626	501	207	7	0	0	0	0	0	0	0	0	0	0
4	0	0	0	0	0	0	0	0	0	2	63	197	666	774	618	218	43	1	0	0	0	0	0	0	0	0	0
5	0	0	0	0	0	0	0	0	0	10	79	226	641	922	557	242	57	12	0	0	0	0	0	0	0	0	0
6	0	0	0	0	0	0	0	0	4	26	58	192	642	876	659	206	55	13	4	0	0	0	0	0	0	0	0
7	0	0	0	0	0	0	0	2	3	14	51	188	581	869	589	174	50	16	2	1	0	0	0	0	0	0	0
8	0	0	0	0	0	0	0	0	4	5	51	143	547	882	524	188	48	20	4	1	0	0	0	0	0	0	0
9	0	0	0	0	0	0	0	1	4	15	60	142	503	836	516	151	53	10	1	1	0	0	0	0	0	0	0
10	0	0	0	0	0	0	1	1	2	10	35	141	472	776	455	135	44	12	2	0	0	0	0	0	0	0	0
11	0	0	0	0	0	0	0	0	1	17	34	127	415	680	405	126	25	12	2	1	0	0	0	0	0	0	0
12	0	0	0	0	0	0	1	0	4	7	28	88	379	645	408	115	25	9	2	1	0	0	0	0	0	0	0
13	0	0	0	0	0	0	0	0	3	1	22	93	352	589	325	93	23	4	1	0	0	0	0	0	0	0	0
14	0	0	0	0	0	0	1	1	4	4	27	77	302	564	324	77	22	1	1	0	0	0	0	0	0	0	0
15	0	0	0	0	0	0	0	0	1	3	22	77	281	518	256	65	17	6	0	0	2	0	0	0	0	0	0
16	0	0	0	0	1	0	0	0	1	6	12	64	238	496	256	68	16	3	1	1	0	0	0	0	0	0	0
17	0	0	0	0	0	0	0	0	1	2	11	48	249	478	204	61	13	2	0	0	0	0	0	0	0	0	0
18	0	0	0	0	0	0	0	1	0	3	9	43	216	413	219	59	15	3	2	0	0	0	0	0	0	0	0
19	0	0	0	0	0	0	0	0	0	2	10	40	202	422	212	50	14	2	0	0	0	0	0	0	0	0	0
20	0	0	0	0	0	0	0	1	2	3	9	38	162	409	175	47	8	0	0	0	0	0	0	0	0	0	0
21	0	0	0	0	0	0	1	0	0	1	9	33	166	350	179	35	9	1	1	0	0	0	1	0	0	0	0
22	1	0	0	0	0	0	0	0	1	4	9	30	170	329	179	40	16	3	3	1	0	0	0	0	0	0	0
23	0	0	0	0	0	0	0	0	0	0	4	19	152	349	132	22	9	1	1	0	0	0	0	0	0	0	0
24	0	0	0	0	0	0	0	0	1	1	10	30	126	337	124	33	4	3	1	1	0	0	0	0	0	0	0
25	0	0	0	0	0	0	0	0	0	1	6	20	97	308	134	29	6	1	3	0	0	0	0	0	0	0	0
26	0	0	0	0	0	0	1	0	1	0	6	20	101	276	139	20	8	0	0	0	0	1	0	0	0	0	0
27	0	0	0	0	0	0	0	0	1	1	4	21	110	256	95	19	7	2	2	0	0	0	0	0	0	0	0
28	0	0	0	0	0	0	0	0	0	1	4	16	88	270	100	20	5	0	0	0	0	0	0	0	0	0	0
29	0	0	0	0	0	0	0	2	0	2	3	14	77	222	93	12	4	0	0	0	0	0	0	0	0	0	0
30	1	2	0	1	0	0	0	0	0	1	3	19	87	240	72	18	4	3	0	0	0	0	0	0	0	0	0
31	1	0	0	0	0	0	0	0	2	2	4	14	76	235	77	6	1	2	0	0	0	0	0	0	0	0	0
32	0	0	0	0	0	0	0	0	1	0	2	14	63	210	79	24	4	1	1	0	0	0	0	0	0	0	0
33	0	0	0	0	0	0	0	0	0	1	2	9	54	203	80	8	4	0	1	0	0	0	0	0	0	0	0
34	0	0	0	0	0	0	0	0	0	1	5	11	73	173	64	10	2	4	0	0	0	0	0	1	0	0	0
35	0	0	0	0	0	0	0	0	2	0	2	8	56	175	56	8	3	0	1	0	0	0	0	0	0	0	0
36	0	0	0	0	0	0	0	0	1	0	3	4	56	165	49	9	3	0	0	1	0	0	0	0	0	0	0
37	0	0	0	0	0	0	0	0	0	0	1	3	42	169	44	8	4	0	0	1	0	0	0	0	0	0	0
38	0	0	0	0	0	0	1	0	0	0	0	7	56	166	35	7	1	0	0	0	0	0	0	0	0	0	0
39	0	0	0	0	0	0	0	1	0	0	2	8	42	138	57	11	1	0	0	0	0	0	0	0	0	0	0
40	0	0	0	0	0	0	0	0	0	0	1	3	53	161	32	7	0	1	0	0	0	0	0	0	0	0	1
41	0	0	0	0	0	0	0	0	0	1	3	5	34	138	32	7	1	2	1	0	0	0	0	0	0	0	0
42	0	0	0	0	0	0	0	0	2	0	1	4	24	133	30	6	1	0	0	0	0	0	0	0	0	0	0
43	0	0	0	0	0	0	0	0	1	3	2	6	27	161	29	2	1	0	0	0	0	0	0	0	0	0	0
44	0	0	0	0	0	0	0	0	1	2	3	5	29	113	25	4	1	3	0	0	0	0	0	0	0	0	0
45	0	0	0	0	0	0	0	0	0	0	1	9	22	118	26	9	2	0	0	0	0	0	0	0	0	0	0
46	0	0	0	0	0	0	0	0	0	0	2	4	29	118	26	3	0	1	0	0	0	0	0	0	0	0	0
47	0	0	0	0	0	0	0	0	0	1	0	4	22	120	23	2	1	1	0	0	0	0	0	0	0	0	0
48	0	0	0	0	0	0	0	0	1	1	1	2	15	99	27	6	0	3	1	0	0	1	0	0	0	0	0
49	0	0	0	0	0	0	0	0	0	1	0	4	27	112	26	5	1	1	0	0	0	0	0	0	0	0	0
50	0	0	0	0	0	0	0	0	0	0	0	1	17	104	20	1	3	0	0	0	0	0	0	0	0	0	0
51	0	0	0	0	0	0	0	0	0	0	1	1	20	87	21	3	2	0	0	0	1	0	0	0	0	0	0
52	0	0	0	0	0	0	0	0	0	0	1	2	15	99	22	2	0	0	1	0	0	0	0	0	0	0	0
53	0	0	0	0	0	0	0	0	0	0	0	1	22	99	20	1	0	0	0	0	0	0	0	0	0	0	0
54	0	0	0	0	0	0	0	0	0	0	0	2	17	87	16	4	2	1	0	1	0	0	0	0	0	0	0
55	0	0	0	0	0	0	0	0	0	0	0	4	8	84	11	3	0	0	0	0	0	0	0	0	0	0	0
56	0	0	0	0	0	0	0	0	0	0	1	0	14	84	17	0	1	0	1	0	0	0	0	0	0	0	0
57	0	0	0	0	0	0	0	0	0	0	0	1	9	76	16	1	0	0	0	0	0	0	0	0	0	0	0
58	0	0	0	0	0	0	0	0	0	0	0	1	8	78	8	1	2	0	0	0	0	0	0	0	0	0	1
59	0	0	0	0	0	0	0	0	0	1	0	0	17	91	10	1	0	0	0	0	0	0	0	0	0	0	0
60	0	0	0	0	0	0	0	0	0	0	0	0	8	67	10	0	1	0	0	0	0	0	0	0	0	0	0

Table 4-3: Sub-regulation ramp events in tabular form
(These values were used in creating the contour plot in Figure 4-17)

Ramp Influence on Voltage

In section III-F the high ramp rates of irradiance were shown to be smoothed out by the spatial distances across the solar facility resulting in much lower power ramp rates. This conclusion was also supported in the discussion on ramp rates in the regulation and sub-regulation series. However, the most important question that needed answered was, "How do the power ramps and ramp rates affect the system voltage which ultimately affects the customer?"

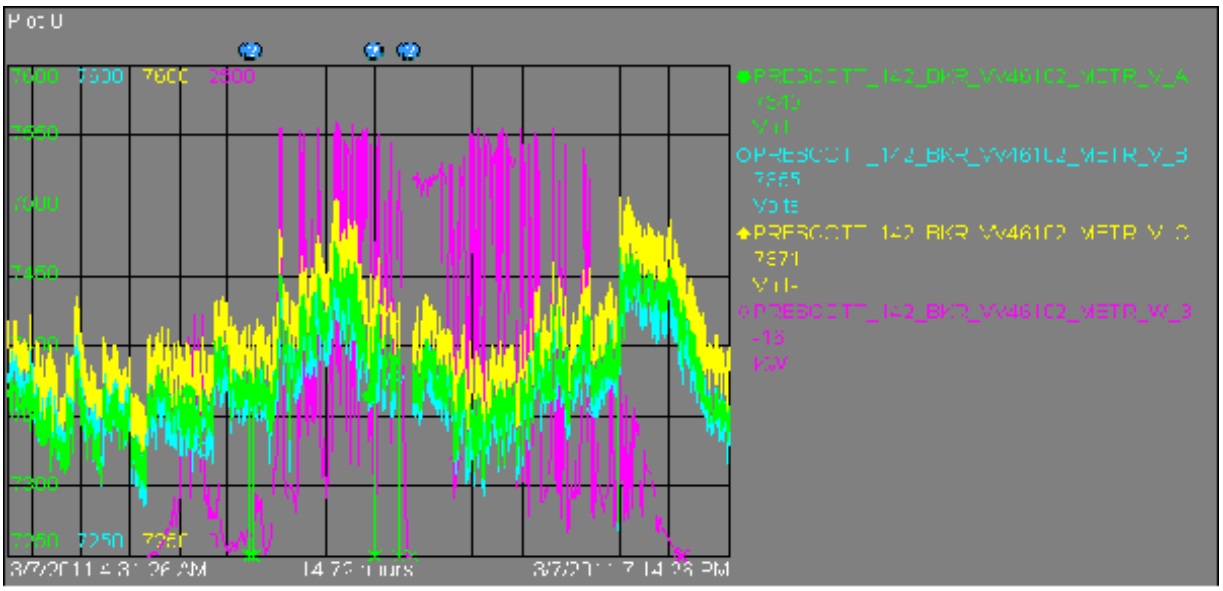

Figure 4-19a: Voltage and Power for March 7

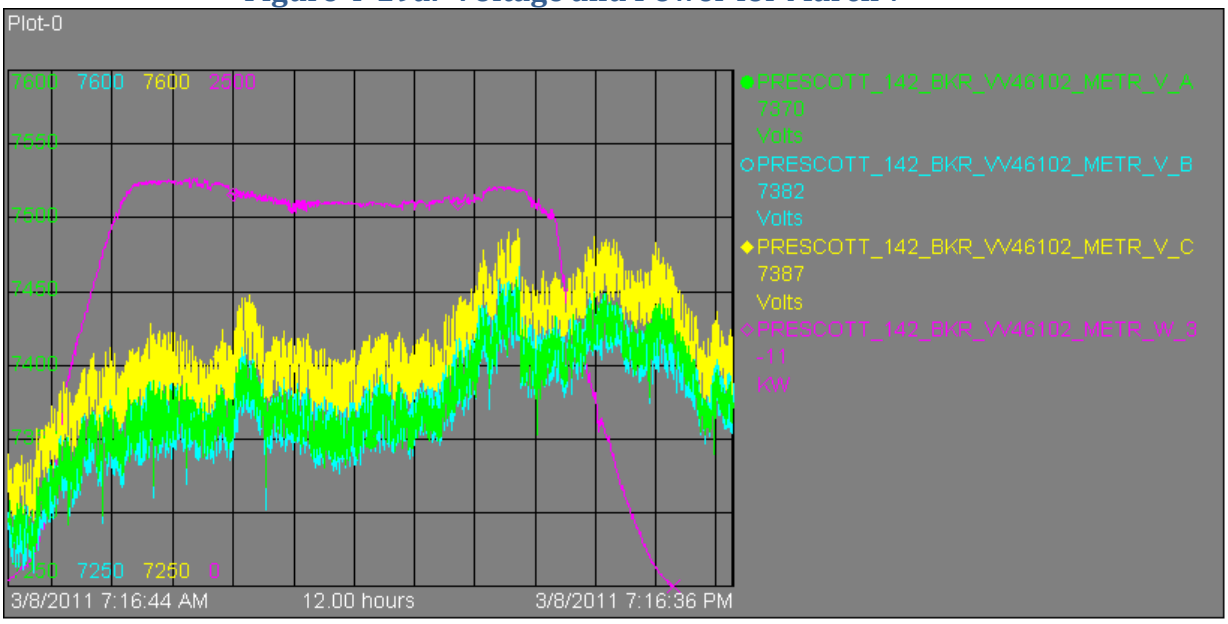

Figure 4-19b: Voltage and Power for March 8

In Figure 4-19a the highly variable power example of March 7 shows that the facility voltage increases and decreases throughout the day by as much as 200 volts peak to peak (green line, Phase A volts); however, the short term voltage swings that may be a result

of variability are never more than about 50 volts peak to peak (green line, Phase A volts). In truth, it is very difficult to differentiate causes for average common output voltage in that many of the changes can be caused by the load on the substation transformer, capacitor switching, or voltage changes on the 69 kV system feeding the substation. In fact, it was questioned whether the voltage swings were tied to variability or were normal variations on the system, particularly when looking at Figure 4-19b which is for March 8. (Note: It can be seen on this graph that there were about five momentary loses of power, sharp spikes downward, to the instrumentation during this period. These events were eliminated in the data analyses that follow.) While there was some instrumentation available on the Energy Management System (EMS) for all these points, no significant effort was placed on trying to correlate these voltages since the real purpose of the study was to correlate variable irradiance to power and power variability or ramps to voltage changes. However, a review of the EMS data (1 minute) taken from SEL351 relay information showed that the solar facility common output voltages (feeder no. 10), the load feeder voltages (feeder no. 12), and the substation voltages were always identical. This led to the conclusion that any transient seen at the solar facility or at the load feeder would influence the other even though the solar facility was located about 2 miles from the interconnect substation . Note that the voltage variations on this clear day are very similar to those that appear during a highly variable, partly cloudy day. While visual verification from the PI charts can demonstrate either corresponding correlations or randomness between power variations and voltage variations, an analysis of the 1-second data from the month of April, 2011 was conducted. In this analysis, all power ramps were collected and then compared to their corresponding, if any, voltage changes. With a more detailed comparison, voltage changes were shown to occur with power variability but not consistently. Several examples of voltage changes correlated to power ramps are shown in Figure 4-20.

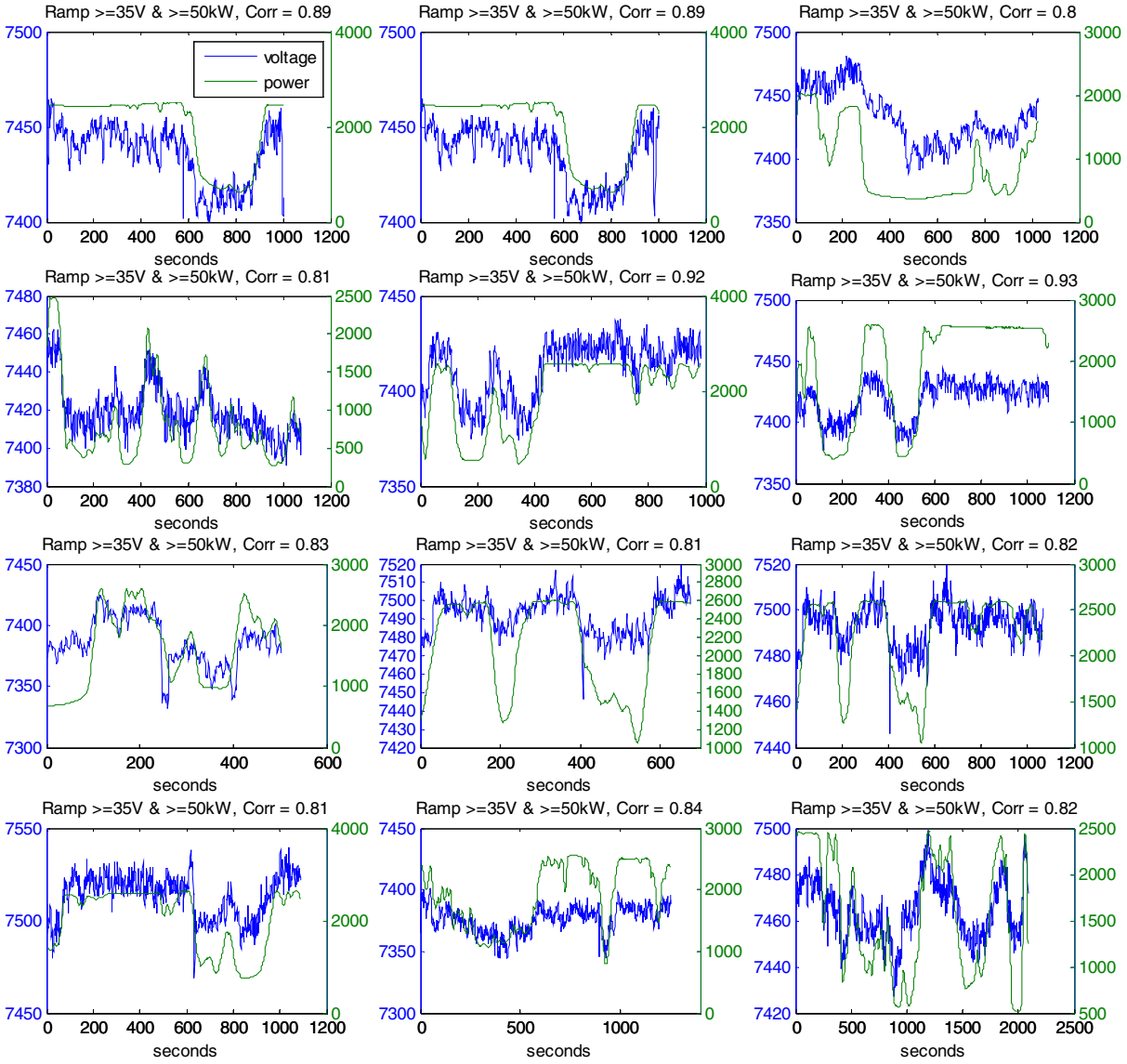

Figure 4-20: Examples of voltage ramps larger than 35V (~0.5% of average voltage)

Note that the voltage changes are for power ramps in excess of 50 kW coinciding with power fluctuations larger than 50kW (~2% of rated capacity). From the examples it can be observed that the amount of variation is dependent on the initial power level of the facility and the size of the power ramp in these cases; however, not all voltage ramps were caused by the facility. A parallel feeder on the substation that is connected to loads, as noted in the system description section, contains two switchable capacitors; one bank operates off both time and voltage, the other bank operates off voltage. In the analysis, there were several capacitor bank voltage events captured. Figure 4-21 shows one of these events.

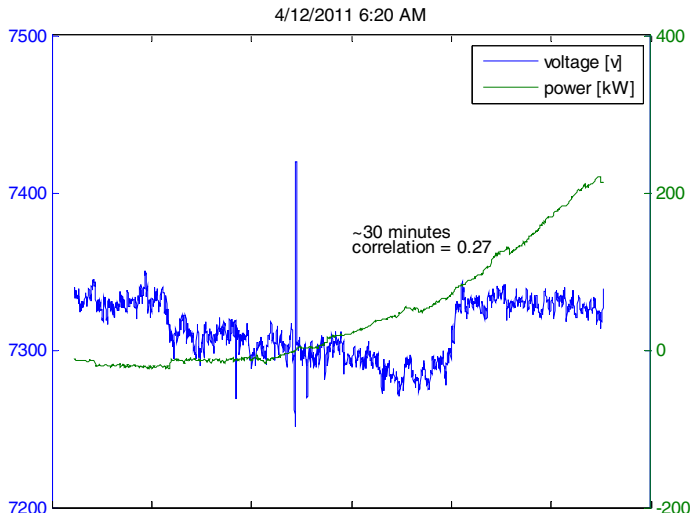

Figure 4-21: Capacitor Switch at Low Voltage

Another facility related voltage ramp event is shown in Figure 4-22 is caused by a partial loss of the facility, about 30%, probably from the trip of two inverters simultaneously. The resultant voltage ramp is only 90 volts.

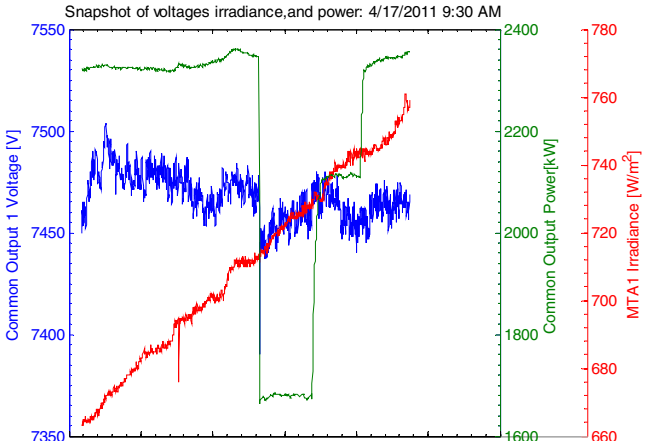

Figure 4-22: Inverter Loss Induced Voltage Ramp

The month of April witnessed the variety of the weather patterns from clear sky, to overcast and rain, and, in particular, several days of scattered clouds. When the data are analyzed over the entire month, even though there were significant power ramp events, there were no instances of voltage violations. While there were a small number that were as much as 150 volt change or 2%, almost all were below 75 volts which is insignificant within the regulation band. Additionally, the ramp rates were consistently small. This is shown in figure 4-23.

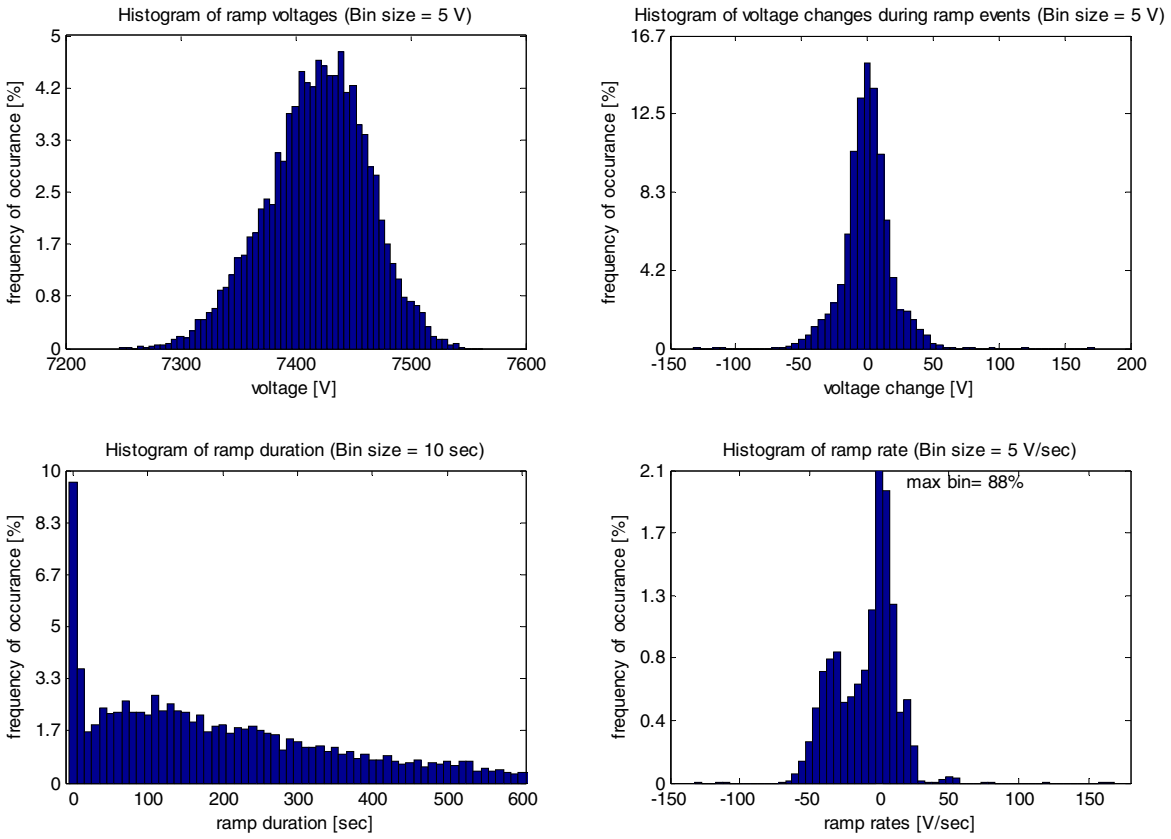

Figure 4-23: Voltage ramp changes and rates corresponding to power ramp events

In conclusion, while there were a number of power change ramps that were in excess of 7%/ second, all induced voltage changes were less than 5% which is well within the regulation requirements of the substation.

Summary of Variability on Solar Facility Output

In this section the output was analyzed to determine the irradiance variability effects on the solar facility output. In particular, the size, duration, and rate of the power ramps were evaluated over a three month period; February, March, and April of 2011. One second data was used to provide sufficient granularity to characterize these ramps into either a regulation or sub-regulation series. After the power ramps were analyzed, efforts were made to correlate power ramp events with voltage change events to determine if a) the voltage events were caused by the power ramps, and if so, b) how large the voltage change events were, and c) if any voltage events caused events beyond the regulation requirements demanded of the substation system.

- The three month period covered a wide range of variability weather conditions providing valuable data.
- The three month period also covered the change from lower irradiance conditions to near peak output conditions due to the sun angle changes.
- 99.7% of all ramp rates were less than 7%/sec.
- The average absolute value of all ramp rates was 13 kW/sec
- There were instances of significant ramp rates (-413 kW/sec downramp and +217 kW/sec upramp); however, the duration was small and resulted in relatively small changes in power.
- Of all ramp events, most of the events were between 1 and 30 seconds.
- Of these events, the large majority of actual power changes were between -50 kW and +50 kW with almost all of the power changes between -500 kW and + 500 kW.
- April, 2011 data was selected to determine correlation between power ramps and voltage change events/ ramps.
- April covered a wide range of variability weather conditions providing valuable data.
- EMS data showed that the solar facility voltages, the load feeder voltages, and the substation voltages were always the same, so that if any voltage event occurred at the solar facility (or vice versa), that change would be seen at the other two locations.
- For all power ramp events occurring within April, all voltage changes were within the 5% regulation requirements for the substation.
- An insignificant number of power ramps induced solar facility voltage changes 2% or greater.

V. FORECASTING

Background

During the process of recording data for each day, 3TIER, Inc. also provided a daily, day ahead graphic forecast for the Prescott Solar site backed up with a 10-minutely data spreadsheet. The forecast was provided for a four month period from March 1 through June 30, 2011. While the forecast was not used for dispatching the plant in anyway, the purpose of the forecast was to compare the day ahead forecast profile with the actual profile of the facility and determine if variability would also be predicted in the forecast.

While much of the analysis conducted by 3TIER is protected under agreement with APS, there were some interesting observations made with the forecast and some interesting correlations with the observed data and NAU analysis of the variability that will be discussed here.[7]

The primary tool for predicting weather, clouds, and thus solar irradiance beyond about six hours is Numerical Weather Prediction (NWP) models. These physics-based models are capable of skillfully estimating the future state of many weather parameters that are important for predicting solar power output. Global Horizontal Irradiance (GHI) at the earth's surface is the primary model output variable that can be used either directly or as an input to other models to produce a power forecast. The conversion from GHI (in W/m^2) to power is not trivial in most cases and depends, in part, on the solar technology and geometry for each specific installed facility.

One of the limitations with using the raw GHI forecast from an NWP model is that systematic biases and imperfect representation of small scale features that can cause local cloudiness are rather pronounced. Errors at fine scales are also compounded by larger scale issues such as the temporal or spatial displacement of cloud structures associated with extratropical cyclones, for example. To overcome inherent systematic model biases, historical irradiance observations at the site can be used to calibrate the raw model forecasts.

Observational data can come from ground instrumentation such as a pyranometer. These measurements come in varying degrees of quality depending on the instrumentation and how it's maintained over time. Oftentimes a promising potential site for a solar energy plant does not have an extensive historical record of on-site ground-based measurements of GHI. This is not only important for determining the long term economic returns from site energy production, but for capturing seasonal to annual scale irradiance variability critical to fine tuning NWP model output for real-time forecasting applications. Irradiance data derived from visible satellite imagery can augment the ground-based measurement or provide the measurement record where none exists.

Method Used for Prescott Solar Forecast

The NWP model forecasts used in this prototype are from the National Centers for Environmental Predictions (NCEP) Global Forecast System (GFS) 0000 UTC cycle. We present results for the next day forecast which is a common time horizon for scheduling renewable energy integration.

Model Output Statistics (MOS) is employed for fine-tuning the NWP GHI forecast. MOS is a stepwise multivariate linear regression model that is very effective at removing bias in model forecasts (Glahn and Lowery, 1972)[8]. The MOS predictors come directly from the NWP day ahead forecasts for a 5-year training period (1/1/2006-12/31/2010). The clearsky Global Horizontal Irradiance (GHC) is also calculated for each hour of the day for every day of the year. This way the clearness index, Kt = GHI/GHC, may be used as both a MOS predictor and predictand.

Observation data utilized by the forecast system to generate the forecast is from 3TIER's Satellite GHI Timeseries. The data set has been well calibrated against a ground observation network, comes at very high spatial resolution (~3 km) and is continuous in time. The satellite-to-irradiance model is based on Perez et al. (2002)[9] and is applied globally for the period 1997-2010. Over the continental U.S., visible imagery from the Geostationary Operational Environmental Satellite (GOES) East and West are used for the calculation of irradiance.

Validation

The forecasts were validated against observations from the Prescott site that were obtained from APS and NAU. Day ahead GHI forecasts at an hourly timestep were compared against hourly averaged observations of GHI from the period March 2011 through June 2011. Errors associated with a baseline, unskilled persistence forecast are also shown for comparison purposes. Persistence assumes the most recent observation of irradiance for a specific hour will be observed the next day for that same hour. For example, the persistence forecast for 3pm tomorrow is based on the observed irradiance at 3pm yesterday.

Not surprisingly, the persistence forecast exhibits large RMS errors as large absolute errors associated with clouds will be penalized heavily (Figure 5-1). The persistence forecasts have a small bias but exhibit the largest MAE and RMSE. The MOS corrected forecasts tend to overpredict clear conditions, but RMSE improvement over persistence is about 50%. The MOS corrected forecast is more skillful than a persistence forecast when looking at bulk error statistics.

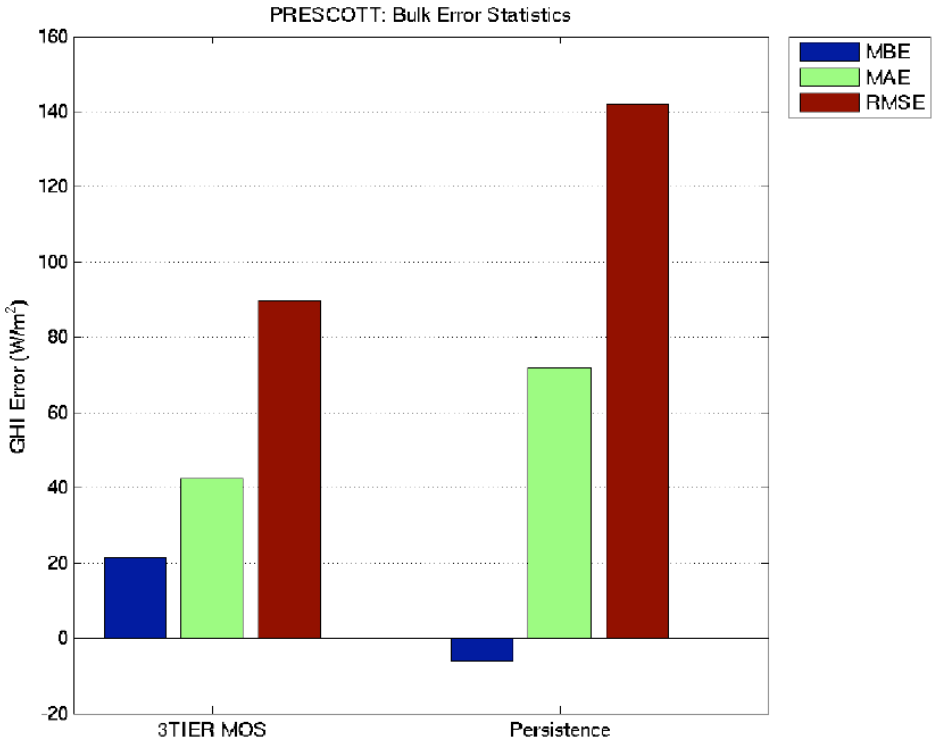

Figure 5-1: Day ahead solar forecast error statistics covering March through June 2011 for Prescott, AZ. Mean Bias Error (MBE), Mean Absolute Error (MAE), and Root Mean Square Error (RMSE) are shown for MOS and Persistence forecasts

The bulk error statistics alone do not reveal when the use of historical observations for generating a MOS forecast adds the most value. Another way to view the forecast performance is by summing up the individual hour-by-hour errors cumulatively (Figure 5-2). What becomes immediately apparent is that the MOS forecast adds more value over an unskilled GHC (clear sky) or persistence forecast at the Prescott location. The individual black tick marks of Figure 5-2 show the hourly advantage (or disadvantage) of the MOS forecast against persistence.

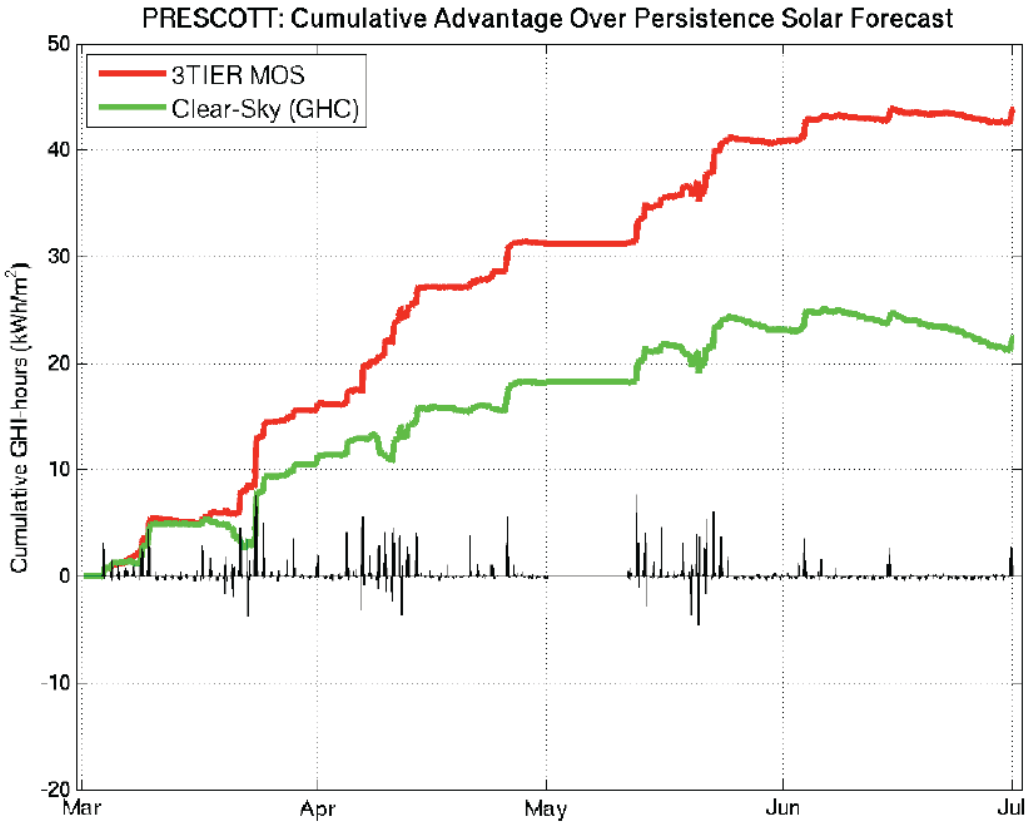

Figure 5-2: Cumulative Advantage (in kWh/m2) for March through June 2011 at Prescott, AZ. Individual black tick marks along "0" axis represents hourly advantage (or disadvantage) of MOS forecast versus persistence

The accumulated MOS forecast advantage over persistence at Prescott is about 45 kWh/m2 over the 4-month validation period. Just as important, the MOS advantage over GHC at Prescott is about 20 kWh/m2. The decrease in cumulative advantage of the GHC forecast towards the end of the period is due to the long period of clear-sky days where the GHC forecast shows a slight high bias. This plot also illustrates how during extensive periods of clear sky where there are small or no black tick marks the 3TIER forecast does a good job at forecasting full production days.

Additional Observations and Postulations Concerning Forecasting:

While 3Tier provided hourly forecasting for the interest of comparison to actual facility output and comparison of methods for solar forecast, the study also evaluated the variability characteristics of the solar facility under a variety of different conditions. This led to a classification method for variability. While as yet untested in application, this method will warrant further refinement and investigation as a possible aid in scheduling generation resources to address potential variable conditions caused by the PV.

Revisiting Section III on Variability, *Natural Variability of Power (NVP)*: Equals the standard deviation of the changes in total power from one data point to the next, divided by the mean of the total power.

$$\boxed{NVP = \frac{\sigma_{\Delta P}}{\bar{P}}} \quad \text{(Eq. 3-3)}$$

Figure 5-3 is a series of graphs showing the hourly variability of power for each day in the month of March 2011.

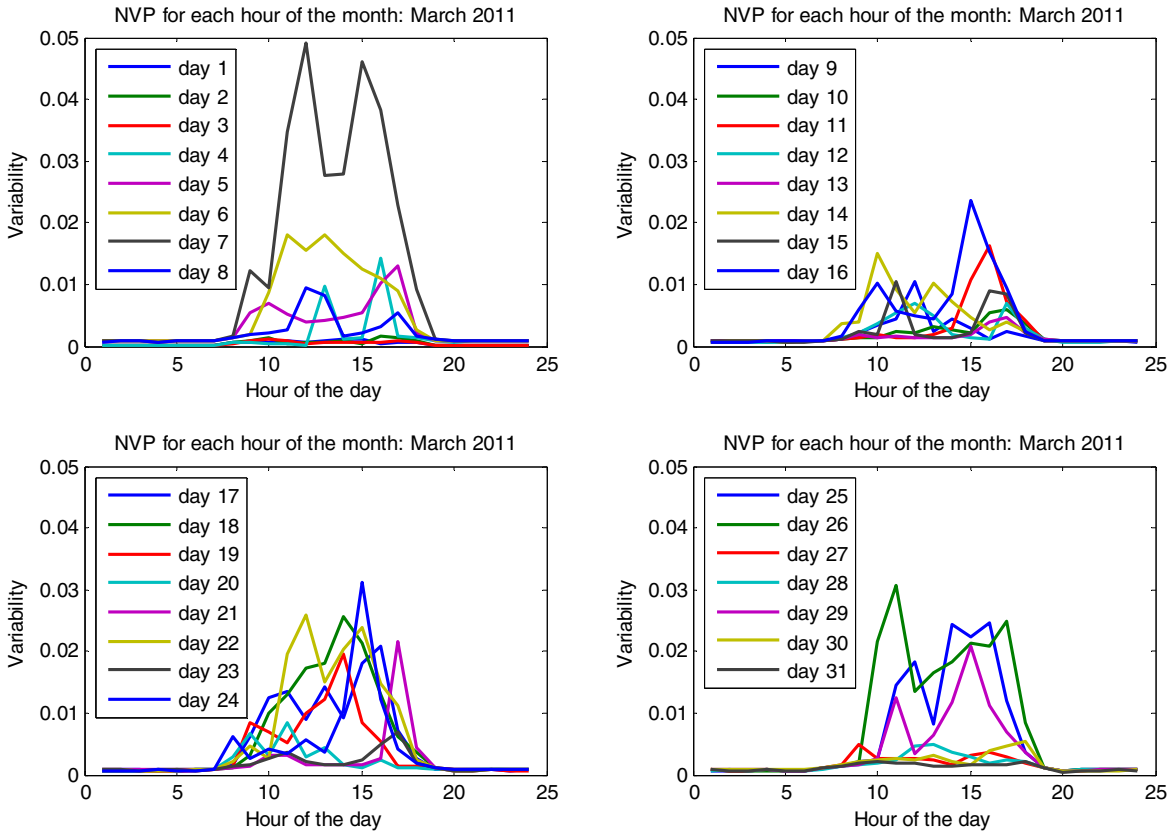

Figure 5-3: Hourly NVP computations using 1-second data: March 2011

These graphs depict the historical data of actual performance and not a forecast, so the question was asked if the historical data could be used to improve forecast performance. This could be done using the NVP ratio to determine a classification system for each degree of variability. This was done using the March data as an example and is shown in Table 5-1 below with an example of each type of NVP class shown in Figure 5-4 .

NVP class 1:	<0.0025
NVP class 2:	0.0025-0.005
NVP class 3:	0.005-0.01
NVP class 4:	>=0.01

Table 5-1: Preliminary NVP Classification based on 1-second data

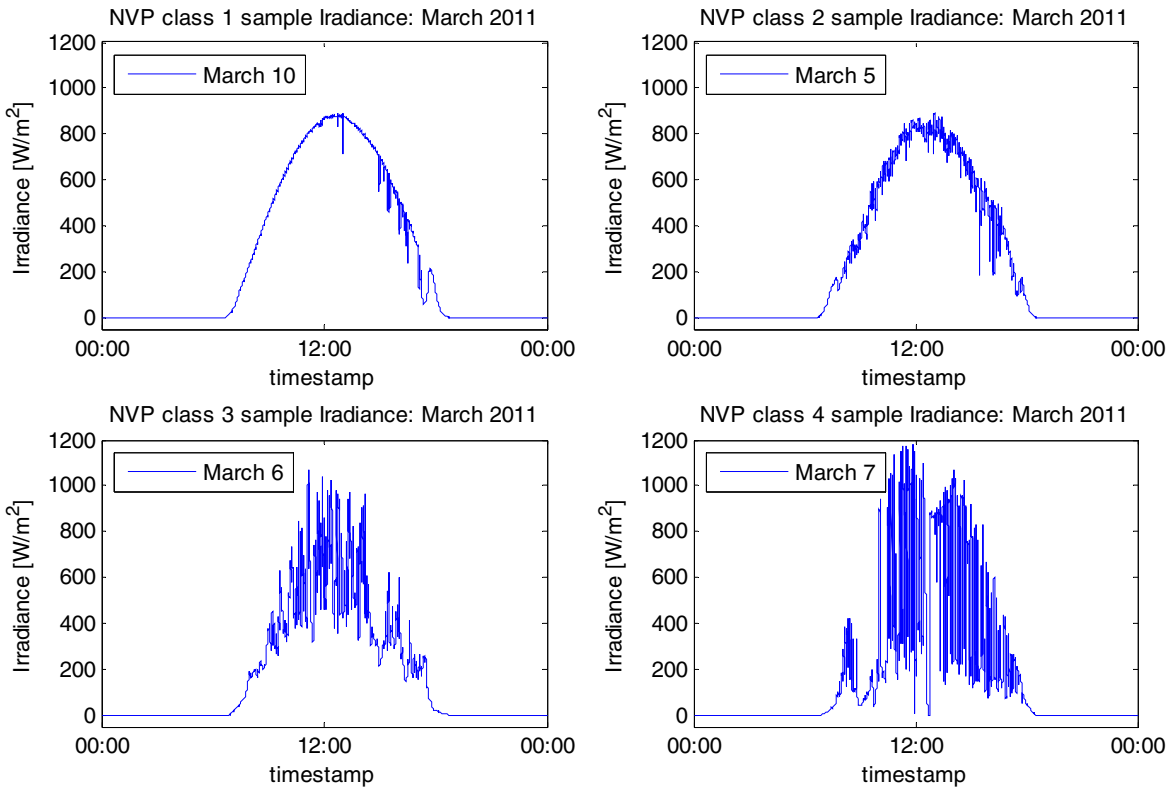

Figure 5-4: Plots showing irradiance values from each NVP Class

The data and figures shown are specific to Prescott, and the classification methodology is a very preliminary postulate based on historical data. However, by drawing a correlation from historical days to forecasted conditions, a more probable level of variability could be achieved and specify a generation strategy that may need to be scheduled to provide reserve and regulation needs accordingly. While there may be sufficient data and tools available to schedule on a day ahead basis, this would more than likely use the classification to determine a confidence factor or margin for error band around a forecast. Many questions remain on the quality of hourly accuracy on a day ahead basis. As discussed above, the current forecasting methods do provide an advantage over persistence and are useful; however, the advantage demonstrated was in the accuracy of the average energy over the hour but not in the variability prediction which is of concern in planning and managing the generation resources. Also note that the most variable day in March, 2011 was forecasted as a mostly sunny day with high, variable clouds. This study was limited in determining any accuracy of forecasting both average energy and variability of the irradiance reaching the ground or solar production equipment and only demonstrated the need for much more detailed analysis in this area. But it is also recognized that there is much work being conducted and considered for establishing metrics of performance and analysis for improvements to the forecasting of cloud and weather induced solar irradiance behavior.

Summary of Forecasting

There was effort in this study to evaluate the state of forecasting and additional ideas that might improve current solar forecasting methodology. The purpose of this effort was not to provide a method for the use of solar forecasting, in its current state, for planning generation but has identified some facts, postulates, and ideas for further study.

- There are limitations on the availability of quality historical, on-ground weather data to help capture seasonal to annual irradiance variability.
    - Improving ground based weather measurement would improve forecasting
    - Satellite data can augment ground based measurement or provide record data where none exists
- While other methodology is still being considered for solar forecasting improvements, MOS forecast provided more value over both persistence and GHC (clear sky) for the hourly average energy and over the period of testing.
- There could be value in forecasting variability for generation regulation requirements through NVP classification methodology or similar variability ratio analysis.
- Local cloudiness and aerosol conditions complicate any GHI forecasting, and all methods require improvement in the capability to forecast cloud formation, type, speed and direction or localized conditions that affect irradiance reaching the ground.

APPENDIX A: POWER CURVE

The APS Prescott Airport Solar Facility was developed as a testing facility and in stages and therefore has a variety of manufacturers and models of solar panels and inverters that have been installed. In addition there is a combination of types of single axis tracking as well as fixed mount. No power curve was ever derived for the facility, and with the variation, could not be derived in the traditional fashion. NAU utilized test data to derive this curve. This was necessary to allow for certain further analyses performed in this study as well as provide a benchmark to 3Tier for the forecasting analysis. Since most facilities would be able to use more traditional methods to derive curves or power data consistent with expected seasonal and locational irradiation data, the methodology to achieve a power curve for this facility is discussed here to document our process.

The first attempt in characterizing the site power output used all data available. It became evident very quickly that this would not provide curves suitable for use without a very sophisticated averaging or curve smoothing as Figure A-1 shows.

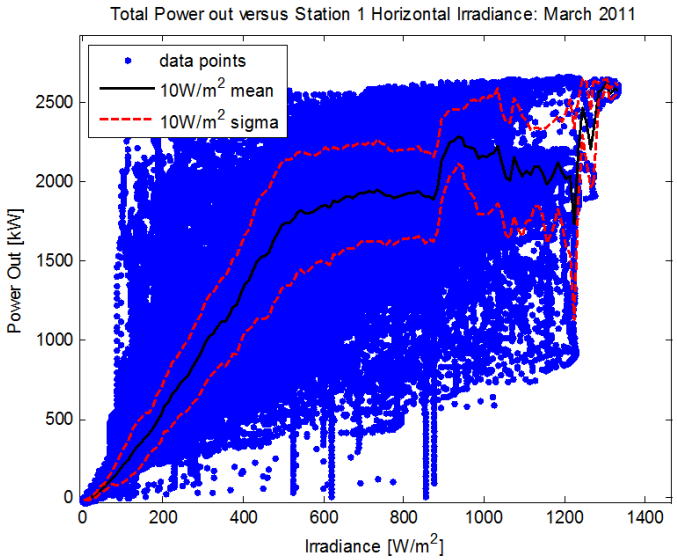

Figure A-1: Initial power curve based off monthly historical data; March 2011

In addition, since the angle of incidence changes on a single-axis tracking system throughout the day, and more importantly from day to day throughout the year, it became evident that daily power curves (or a single POA curve with daily POA/GHI ratios) would be required in order to provide a forecasting company such as 3TIER the information required to accurately forecast power production for all hours of the year. Another approach would be to use a procedure that would to subdivide the power output into 10 W/m^2 bins to devise an average power curve that might be used each day of the year regardless of the variability. Figure A-2 shows the variability of the output for March 7, a cloudy day. By using the binning procedure and calculating the mean output power, the result is shown in Figure A-2 and demonstrates a large degree of uncertainty. The large scatter in the data shown in Figure A-2 along with the choppy nature of the mean power curve is due to a number of factors:

1. The proximity of the irradiance measurement to each array of panels used at the power plant. Thus, the measured irradiance may be significantly different than the mean irradiance to which each array of panels is exposed.
2. The reaction of the inverters to the panel output variability. Each type of inverter may respond differently to the rapid changes in PV panel output as clouds pass.
3. The number of data points within the 10 W/m^2 bins during that day used to generate the power curve may not have a large number of data points, potentially leading to relatively large changes in power output from one bin to the next (making the curve "choppy").

Additionally, due to the sun angles inherent in a single-axis tracking system, the power plant was also capped at about 2500 kW due to the limitations of the individual inverters, resulting in the "spilling" of energy during the months of April-September. The result of this was a decrease in variability during the time of the year/day that power can generate more energy than the inverters are rated for similar to a wind turbine operating between its rated and cutoff wind speeds.

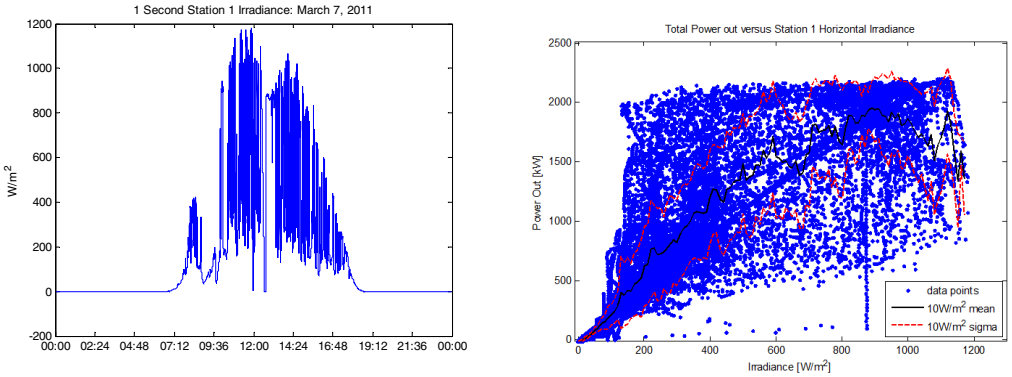

Figure A-2: Left, GHI vs. time of day; Right, power output data (blue) and power curve (black line) on a relatively cloudy day: March 7 2011

With these issues it was evident that a different approach was necessary. Simplistically, clear or relatively clear days provide the best and most consistent data to characterize the true nature of the facility. March 8, 2011, a relatively clear day but with some evidence on the scanner of periodic, very high level moisture clouds, is shown in Figures A-3 with accompanying picture from the scanner. The differences between these figures and the cloudy day of March 7 in Figures A-2 are significant in that a much improved power curve is evident.

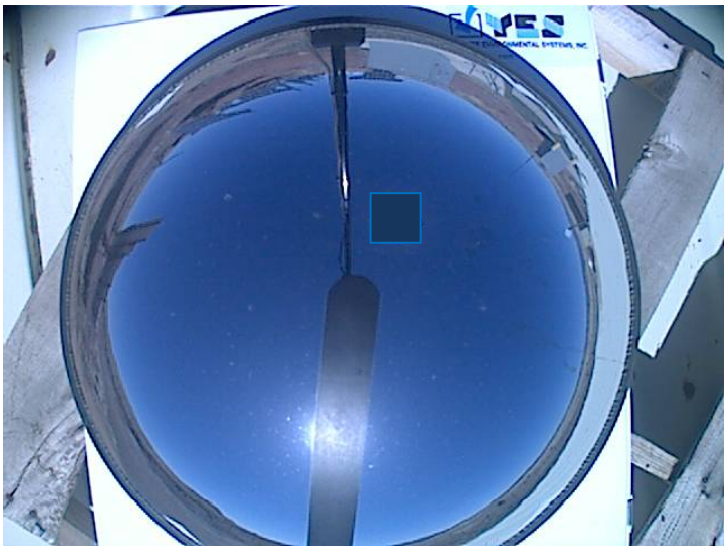

Scanner picture: March 8, 2011 1300

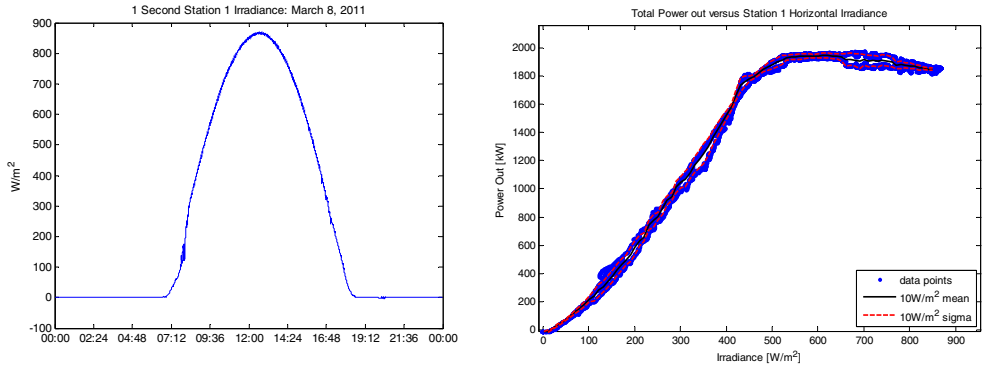

Figure A-3: Left, GHI vs. time of day; Right, power output data (blue) and power curve (black) on a relatively clear day: March 8 2011. A picture from the sky scanner on March 8 is shown above.

Figure A-4 shows the mean power curve for some relatively clear historical days in March 2011, plotted versus the irradiance measured at Station 1. Note the curves in Figure A-4 were generated in the same manner as Figure A-1, but instead of using data from the entire month, each curve was created using data only from that day. Note that the peak power at the end of the month shows a much higher peak power than at the beginning of the month. The month of March shows a marked increase in peak power each day due to the increase in sun angle in relation to the solar facility from the beginning to the end of March. This reflects the obvious that the power curves, day to day, would need to be adjusted with sun angle of the Plane of Array irradiance to power relationship; however, for this test duration, this was not deemed necessary. The power expectation for the day was compared to the closest clear day power curve.

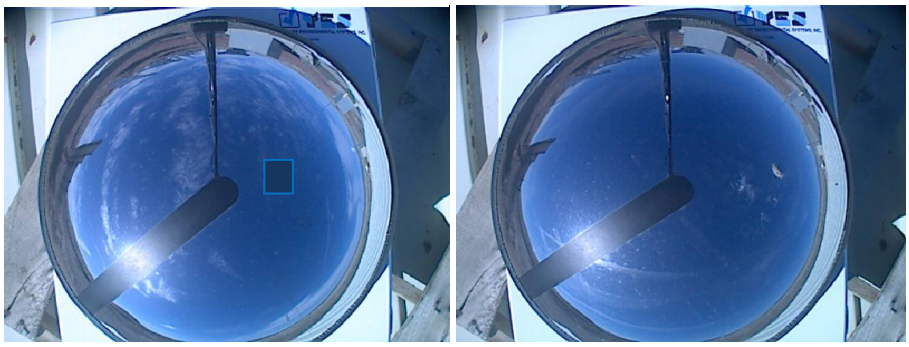

Typical Scanner Pictures for March, 2011

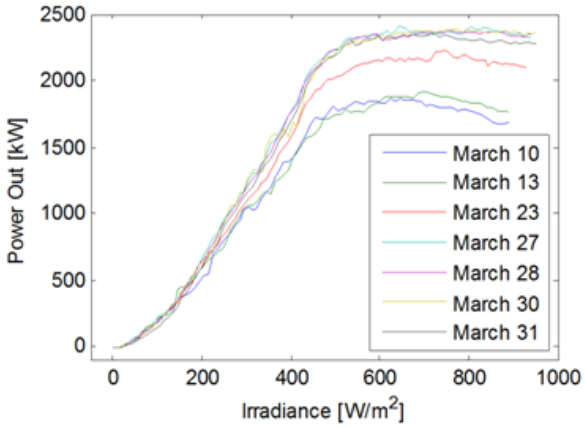

Figure A-4: Power curves for relatively clear days in the Month of March

REFERENCES:

1. Mills, A., Ahlstrom, M., Brower, M., Ellis, A., George, R., Hoff, T., Kroposki, B., Lenox, c., Miller, N., Stein, J., Wan, V. Understanding Variability and Uncertainty of Photovoltaics for Integration with the Electric Power System. LBNL-2855E. December, 2009.
2. ("Comments on presentation materials from Dave Willy", Joshua Stein, Sandia National Laboratories, May, 10, 2011.)
3. Mills, A., Wiser, R. Implications of Wide-Area Geographic Diversity for Short-Term Variability of Solar Power. LBNL-3884E. September, 2010.
4. Horst, J. and Beichl, I. "Efficient piecewise linear approximation of space curves using chord and arc length," *Proceedings of Machine Vision 96*,(1996)
5. Makarov, Y., Loutan, C., Ma, J., De Mello, P. "Operational Impacts of Wind Generation on California Power Systems." IEEE Transaction on Power Systems (2009).
6. EV Systems. (2010). "GE Critical Aperture Convergence – EVSystems Data Solutions." Retrieved August 2010, from EVSystems: www.evsystems.net/files/GE_Historian_Compression_Overview.ppt.
7. Vandervoort, A., Lerner, J. Validation of Global Horizontal Irradiance Forecasts at the Prescott Airport Solar Site. February, 2012.
8. Glahn H.R., Lowry D. a. The use of model output statistics (MOS) in objective weather forecasting. Journal of Applied Meteorology, 11pp. 1203-1211, 1972.
9. Perez R., P. Ineichen, K. Moore, M. Kmiecik, C. Chain, R. George and F. Vignola. A New Operational Ground reference/ Satellite reference Satellite-toIrradiance Model. Solar Energy 73, 5, pp. 307-317, 2002.